

Received: 2 October 2010 – Accepted: 27 October 2010 – Published: 5 November 2010

Correspondence to: K. Toyota (Kenjiro.Toyota@ec.gc.ca)

Published by Copernicus Publications on behalf of the European Geosciences Union.

ACPD

10, 26207–26278, 2010

3-D modeling of Arctic boundary-layer bromine and ozone

K. Toyota et al.

Title Page

Abstract

Introduction

Conclusions

References

Tables

Figures

◀

▶

◀

▶

Back

Close

Full Screen / Esc

Printer-friendly Version

Interactive Discussion



Abstract

Episodes of high bromine levels and surface ozone depletion in the springtime Arctic are simulated by an online air-quality model, GEM-AQ, with gas-phase and heterogeneous reactions of inorganic bromine species and a simple scheme of air-snowpack chemical interactions implemented for this study. Snowpack on sea ice is assumed to be the only source of bromine to the atmosphere and capable of converting relatively stable bromine species to photolabile Br_2 via air-snowpack interactions. A “bromine explosion”, by which Br^- retained in the snowpack is autocatalytically released to the atmosphere as a result of dry deposition of HOBr and BrONO_2 , is assumed to occur on young, first-year (FY) sea ice (or its overlying snowpack), whereas the snowpack on old, multi-year (MY) sea ice and over land is assumed only to recycle a part (but up to 100%) of bromine reservoirs lost via dry deposition back to Br_2 . Model runs are performed for April 2001 at a horizontal resolution of approximately $100 \text{ km} \times 100 \text{ km}$ in the Arctic. The model simulates temporal variations in surface ozone mixing ratios as observed at stations in the high Arctic and the synoptic-scale evolution of enhanced BrO column amounts (“ BrO clouds”) as seen from satellite reasonably well. The results strongly suggest: (1) a ubiquitous source of reactive bromine exists on the FY sea ice during the Arctic springtime; and (2) the timing of bromine release to the atmosphere is largely controlled by meteorological forcing on the transport of ozone to the near-surface air. Also, if the surface snowpack supplies most of the reactive bromine in the Arctic boundary layer, it should be capable of releasing reactive bromine at temperatures as high as -10°C , particularly on the FY sea ice in the central and eastern Arctic Ocean. Dynamically-induced BrO column variability in the lowermost stratosphere appears to interfere with the use of satellite BrO column measurements for interpreting BrO variability in the lower troposphere but probably not to the extent of totally obscuring “ BrO clouds” associated with the surface source of bromine in the high Arctic. Contrary to our original intention, the present air-snowpack interaction scheme yields a majority of atmospheric bromine input via Br_2 release associated empirically with a

3-D modeling of Arctic boundary-layer bromine and ozone

K. Toyota et al.

Title Page

Abstract

Introduction

Conclusions

References

Tables

Figures

◀

▶

◀

▶

Back

Close

Full Screen / Esc

Printer-friendly Version

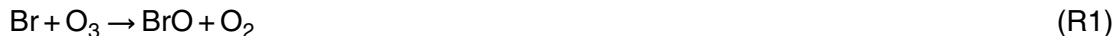
Interactive Discussion



dry deposition of ozone on the snow/ice surface under sunlight to represent a trigger of bromine explosion. This implies that the bromine explosion actually occurs in the interstitial air of snowpack and/or is accelerated by heterogeneous reactions on the surface of wind-blown snow in ambient air, both of which are missing in our model but could have been approximated by a parameter adjustment for the yield of Br₂ from the trigger.

1 Introduction

During the springtime after complete darkness in winter, boundary-layer air over Arctic sea ice and at its surrounding coastal sites experiences the frequent occurrence of ozone depletion events (ODEs) from background levels (~30–40 nmol mol⁻¹) to below 5–10 nmol mol⁻¹ and sometimes even below experimental detection limits ($\lesssim 1$ nmol mol⁻¹) (Oltmans, 1981; Bottenheim et al., 1986, 2002, 2009; Solberg et al., 1996; Hopper et al., 1998; Tarasick and Bottenheim, 2002). The ODEs are generally accompanied by a significant increase in gaseous and particulate bromine abundances (Barrie et al., 1988; Oltmans et al., 1989; Li et al., 1994) and the detection of BrO radicals as high as 30 pmol mol⁻¹ in the boundary layer has provided evidence for bromine radical chemistry in depleting ozone in less than several days (Hausmann and Platt, 1994; Tuckermann et al., 1997):



The boundary-layer ODEs also take place over sea ice around the Antarctica (Yurganov, 1990; Murayama et al., 1992; Wessel et al., 1998; Tarasick and Bottenheim,

3-D modeling of Arctic boundary-layer bromine and ozone

K. Toyota et al.

Title Page

Abstract

Introduction

Conclusions

References

Tables

Figures

◀

▶

◀

▶

Back

Close

Full Screen / Esc

Printer-friendly Version

Interactive Discussion



2002), where the increase of IO radicals to about 20 pmol mol⁻¹ along with BrO radicals indicates a synergistic effect of bromine and iodine radical chemistry on the ozone loss (Kreher et al., 1997; Frieß et al., 2001, 2004; Saiz-Lopez et al., 2007; Schönhardt et al., 2008). Such substantial enhancement in the IO abundance has not been found in the Arctic (Tuckermann et al., 1997; Schönhardt et al., 2008). Satellite measurements have revealed frequent and widespread occurrence of enhanced BrO column amount, called “BrO clouds”, in the polar regions of both hemispheres particularly during the springtime (Chance, 1998; Richter et al., 1998; Wagner and Platt, 1998; Wagner et al., 2001).

Heterogeneous chemistry plays a critical role for the formation of reactive bromine in the polar boundary layer. With a realization that the snowpack retains a significant amount of bromide (Br⁻) originated from seawater and accessible from the atmosphere by wind pumping, the following reactions have been proposed as key steps to a net release of bromine from the snowpack to the atmosphere (Tang and McConnell, 1996; Michalowski et al., 2000; Lehrer et al., 2004):



where HOBr and BrONO₂ are reproduced via gas-phase chemistry in the atmosphere and presumably in the snowpack interstitial air as well, subsequent to the photolysis of Br₂ (Reaction R3) and the production of BrO via Reaction (R1):



These reactions constitute an autocatalytic cycle of releasing bromine from the snowpack to the atmosphere, called “bromine explosion” (Wennberg, 1999), which continues until the production of HOBr and/or BrONO₂ diminishes after ozone is depleted and is

3-D modeling of Arctic boundary-layer bromine and ozone

K. Toyota et al.

[Title Page](#)[Abstract](#)[Introduction](#)[Conclusions](#)[References](#)[Tables](#)[Figures](#)[◀](#)[▶](#)[◀](#)[▶](#)[Back](#)[Close](#)[Full Screen / Esc](#)[Printer-friendly Version](#)[Interactive Discussion](#)

3-D modeling of Arctic boundary-layer bromine and ozone

K. Toyota et al.

Title Page

Abstract

Introduction

Conclusions

References

Tables

Figures

◀

▶

◀

▶

Back

Close

Full Screen / Esc

Printer-friendly Version

Interactive Discussion

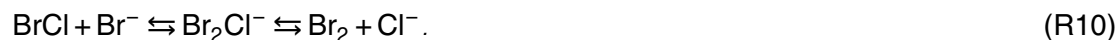


then taken over by the deposition of inactive bromine species perhaps in the form of gaseous HBr and particulate Br⁻ back to the snowpack. Without heterogeneous reactions on aerosols and ice crystals, however, relatively stable HBr formed via reactions between Br-atoms and aldehydes would dominate the partitioning of gaseous inorganic bromine all the time, hindering the build up of reactive bromine and resultant ozone loss (Barrie et al., 1988; Bottenheim et al., 1990; McConnell et al., 1992). In the springtime Arctic, sulfate aerosols of anthropogenic origin may be abundant enough to convert HBr into photolabile Br₂ efficiently via Reactions (R4–R5) for sustaining active bromine chemistry (Fan and Jacob, 1992). An additional influence on bromine chemistry arises from a condensed-phase photochemistry of impurities in the snowpack to release reactive trace gases including NO₂, which is involved in the BrONO₂ formation, and HCHO, which is not only involved in HBr formation but also a precursor of HO₂ involved in the HOBr formation (Grannas et al., 2007).

The chemistry of Br₂ release from salty snow/ice (Reaction R4–R5) often involves Cl⁻, which is typically 2 to 3 orders of magnitude more abundant than Br⁻ in seawater and polar snowpack (Simpson et al., 2005), to give BrCl as an initial step:



followed by halogen inter-exchange reactions (Adams et al., 2002):



A part of BrCl is released to ambient air before reacting with Br⁻ in the snowpack and then undergoes photolysis to produce Cl-atoms along with Br-atoms (Michalowski et al., 2000). The Cl-atoms subsequently destroy hydrocarbons, leading to a substantial variability in their concentrations as observed in the springtime Arctic boundary layer, but are believed to play a marginal role in ozone loss (Jobson et al., 1994; Solberg et al., 1996; Ramacher et al., 1999). High levels of Br₂ and BrCl have been detected

concurrently in ambient surface air and in the interstitial air of snowpack, supporting the occurrence of Reactions (R10) (Foster et al., 2001; Spicer et al., 2002).

Sander et al. (2006) suggested an essential role of low temperature conditions for activating the bromine chemistry in two ways: first, by carbonate precipitation from brine to titrate its alkalinity (more than 80% of carbonate originally contained in sea-water estimated to precipitate when cooled down to -8°C) so that the brine can be acidified by a relatively small amount of acidic gas uptake, and second, by shifting the equilibrium constants of Reactions (R10) towards the Br_2 formation. More recently, however, Morin et al. (2008) argued that the carbonate precipitation should not reduce the alkalinity of brine as proposed by Sander et al. (2006) (see also a follow-up study by Sander and Morin, 2010). At least at temperatures above the freezing point of water, for the release of Br_2 and/or BrCl to occur via uptake of gaseous HOBr , aqueous salt solutions need to be acidified to pHs below 6.5 (Fickert et al., 1999), which would be hardly attainable in the pristine snowpack particularly in the Antarctic. Adams et al. (2002) experimentally showed that the reactive uptake of HOBr onto frozen NaBr/NaCl solution results in the Br_2 and/or BrCl release below -20°C even if the substrate is alkaline at room temperature before frozen.

Fresh, growing sea ice entraps brine, which is expelled from the ice during congelation, and the salinity of brine increases with decreasing temperature (Steffen and DeMaria, 1996; Light et al., 2003). Some brine is also expelled onto the top of sea ice. Under some circumstances, the condensation of water vapor leads to a formation of intricate crystals called “frost flowers”, which wick up salinity from the slurry surface of the sea ice and are then covered with drifting snow in several days (Perovich and Richter-Menge, 1994). Rankin et al. (2002) and Kaleschke et al. (2004) suggested that the frost flowers themselves, either bound to the sea ice or suspended in the air after wind abrasion, provide a major source of reactive bromine to the polar boundary layer. The latter authors proposed an algorithm to diagnose the potential coverage of frost flowers (called “potential frost flower”, or PFF) on sea ice across the polar regions by using satellite data of sea ice concentrations and objective analyses of large-scale surface air

3-D modeling of Arctic boundary-layer bromine and ozone

K. Toyota et al.

Title Page

Abstract

Introduction

Conclusions

References

Tables

Figures



Back

Close

Full Screen / Esc

Printer-friendly Version

Interactive Discussion



temperatures. Their algorithm predicts increased PFF values with decreasing surface air temperatures particularly below -20°C for a given rate of open/refreezing leads formation in the sea ice. Simpson et al. (2007a), however, showed that the PFF data obtained by the Kaleschke et al. (2004) algorithm did not provide a good measure for locating the source of reactive bromine on Arctic sea ice to explain the origins of enhanced BrO columns measured from the ground at Barrow, Alaska. The age of sea ice as to whether it is first-year (FY) or multi-year (MY) can also be retrieved remotely from satellite (e.g., Kwok, 2004). According to Simpson et al. (2007a), the FY sea ice is a better indicator for locating the source region of reactive bromine than the PFF, possibly because salinity is generally higher in the FY sea ice than in the MY sea ice. More recently, Yang et al. (2008, 2010) incorporated the effect of blowing snow as a ubiquitous, airborne source of reactive bromine over Arctic and Antarctic sea ice in their global chemical transport model and reproduced many observed features in BrO column data obtained from space and ground stations.

Readers may refer to recent reviews by Simpson et al. (2007b) and Grannas et al. (2007) for more extensive discussion about ODEs and halogen chemistry in the polar boundary layer as well as about snowpack photochemistry releasing a variety of compounds to the atmosphere. The springtime bromine chemistry is also important for the geochemical cycle of mercury in the polar regions (see Steffen et al., 2008, for a review).

In this study we focus on the surface source problem with regard to the occurrence of high bromine levels and ODEs in the Arctic spring. By using a three-dimensional online air-quality model that incorporates bromine chemistry, it is shown that the outbreak of reactive bromine release initiated mainly on the FY sea ice accounts for surface ozone variability as observed at Arctic coastal stations and even the occurrence of “BrO clouds” as seen from satellite reasonably well, and that they are altogether controlled by synoptic-scale meteorological forcing. The issue of temperature condition required for the reactive bromine release from the snowpack is also addressed by parameter sensitivity experiments.

3-D modeling of Arctic boundary-layer bromine and ozone

K. Toyota et al.

[Title Page](#)[Abstract](#)[Introduction](#)[Conclusions](#)[References](#)[Tables](#)[Figures](#)[◀](#)[▶](#)[◀](#)[▶](#)[Back](#)[Close](#)[Full Screen / Esc](#)[Printer-friendly Version](#)[Interactive Discussion](#)

2 Model description

GEM-AQ is an online air-quality model in which gas-phase oxidant chemistry and size-resolved multi-component aerosol modules are implemented to a Canadian weather forecast model, GEM (Global Environmental Multiscale model). It has been used for simulating the regional-scale transport and microphysical evolution of aerosols released from forest fires (O'Neill et al., 2006), the global distributions of HCN in the upper troposphere (Lupu et al., 2009), and the formation and transport of ozone in the lower troposphere during the summer 2006 heat wave in Europe (Struzewska and Kaminski, 2008). The model has been evaluated also from a perspective of global tropospheric chemistry (Kaminski et al., 2008). Unless otherwise noted, the present model configuration is the same as described in Kaminski et al. (2008).

2.1 Numerical configuration

An important feature of the host GEM model is that it allows global simulations with variable resolution grids by zooming the region of interest (Côté et al., 1998). Results shown here are based on model runs with a global variable grid having a reasonably high resolution over the Arctic Ocean and surrounding subarctic regions. It has 191×150 horizontal grid cells in total, among which 90×90 grid cells around the North Pole comprise a uniform core at $0.88^\circ \times 0.88^\circ$ (approximately $100 \text{ km} \times 100 \text{ km}$) resolution and remaining grid cells spread outside the core by a stretching factor of 1.04 per grid southwards. The vertical grid consists of 28 levels and extends from the ground/sea surface to 10 hPa in a hybrid p - σ coordinate, containing 8 layers in the lowest 2 km. The model accounts for large-scale advection, turbulent diffusion, convective transport, emissions, dry and wet deposition, chemical reactions and aerosol microphysics. Each sub-process is integrated at a time step of 1800 s.

3-D modeling of Arctic boundary-layer bromine and ozone

K. Toyota et al.

Title Page

Abstract

Introduction

Conclusions

References

Tables

Figures

◀

▶

◀

▶

Back

Close

Full Screen / Esc

Printer-friendly Version

Interactive Discussion



2.2 Gas-phase and heterogeneous chemistry

GEM-AQ has incorporated gas-phase oxidant chemistry based on the Acid Deposition and Oxidant Model (ADOM) mechanism (Stockwell and Lurmann, 1989), designed originally for regional air-quality simulations, with a modification made for extended applications to background tropospheric chemistry (Kaminski et al., 2008). The heterogeneous hydrolysis of N_2O_5 on aerosols is also included, for which Canadian Aerosol Module, CAM (Gong et al., 2003), can provide online spatial distributions of five components of size-resolved aerosols, viz. sea salt (produced on the ice-free ocean), sulfate, black carbon, organic carbon, and dust. Among these, only sulfate and sea salt are switched on in our present model runs for numerical efficiency and relevance to Arctic bromine chemistry. The sea-salt aerosols are assumed not to serve as a source of halogens but to provide their surface to facilitate heterogeneous reactions along with the sulfate aerosols (cf. Vogt et al., 1996; Toyota et al., 2004; Yang et al., 2005).

For the present study, we add gas-phase chemistry and simplified heterogeneous chemistry of six inorganic bromine species, viz. Br, BrO, Br₂, HOBr, BrONO₂ and HBr (Table 1). As mentioned in the Note e of Table 1, the Br₂ production in Reaction (G132) is assumed to be controlled by the concurrent uptake of HOBr and BrONO₂ onto aerosols so that the first-order rate constant of HBr loss for Reaction (G132) is adjusted at every time step by diagnosing the availability of HOBr and BrONO₂ from the gas phase. This adjustment procedure, taken together with product assignment for Reaction (G130), serves as a numerically efficient means of approximating the competitive formation of Br₂ and BrCl via Reaction (R10) in our simple scheme of bromine chemistry but without chlorine chemistry. Simulated concentrations of sulfate and sea-salt aerosols are briefly evaluated against ground-level observations from selected Arctic sites (see Sect. S2 in the electronic Supplement).

Zhao et al. (2008) developed another version of GEM-AQ by taking a multiphase chemistry module from Sander et al. (2005) and then simulated reactive halogen release from sea-salt aerosols produced by wind abrasion of frost flowers. The present

3-D modeling of Arctic boundary-layer bromine and ozone

K. Toyota et al.

Title Page

Abstract

Introduction

Conclusions

References

Tables

Figures



Back

Close

Full Screen / Esc

Printer-friendly Version

Interactive Discussion



reaction scheme is less sophisticated in the treatment of heterogeneous reactions but numerically more efficient than that employed by Zhao et al. (2008).

2.3 Emission, deposition, and air-snow/ice surface interactions of reactive bromine species

We use a parameterization for the dry deposition of gaseous compounds to quantify the sink, and the source as explained below, of inorganic bromine species on various types of the Earth surface. GEM-AQ calculates dry deposition velocities by a multiple-resistance approach with aerodynamic, quasi-laminar layer and bulk surface resistances acting in series (Wesely, 1989; Zhang et al., 2002). The surface resistance for each compound is obtained by parametric functions of an effective Henry's law at neutral pH and an estimated oxidative reactivity based on semi-empirical scaling against SO_2 and O_3 (Table 2). Except on the snow/ice-covered surface, dry deposition is assumed to remove HBr, HOBr, BrONO_2 and Br_2 irreversibly from the atmosphere. On the sea ice and snow/ice-covered land surfaces, the surface resistance is reduced to zero for HOBr, BrONO_2 and HBr so that their dry deposition velocities are controlled mainly by aerodynamic resistance and can be as large as about 1 cm s^{-1} when windy but otherwise orders of magnitude smaller in the statically stable Arctic boundary layer. In addition to the dry deposition, HBr is assumed to undergo wet deposition via impaction scavenging in precipitation at a first-order rate constant ($3.89 \times 10^{-4} \text{ s}^{-1}$ per mm h^{-1} of precipitation) as employed in GEM-AQ for HNO_3 (Langner et al., 1998).

The dry deposition of Br_2 is assumed not to occur on the snow/ice covered surface; instead, Br_2 is emitted to the atmosphere at a rate prescribed from the dry deposition fluxes of HOBr, BrONO_2 , HBr and O_3 (Fig. 1). This approach is similar to the one employed by Lehrer et al. (2004) in their one-dimensional model study. The capacity of the Br_2 emission is assumed to vary between the FY and MY sea-ice surfaces and the snow-covered land surface as described below. Following the Simpson et al. (2007a) study, we first assume that the FY sea ice is more efficient at releasing reactive bromine from its overlying snowpack than the MY sea ice.

3-D modeling of Arctic boundary-layer bromine and ozone

K. Toyota et al.

Title Page

Abstract

Introduction

Conclusions

References

Tables

Figures

◀

▶

◀

▶

Back

Close

Full Screen / Esc

Printer-friendly Version

Interactive Discussion



3-D modeling of Arctic boundary-layer bromine and ozone

K. Toyota et al.

Title Page

Abstract

Introduction

Conclusions

References

Tables

Figures

⏪

⏩

◀

▶

Back

Close

Full Screen / Esc

Printer-friendly Version

Interactive Discussion



The snowpack on FY sea ice is assumed to retain an inexhaustible storage of Br^- so that the total dry deposition flux of HOBr and BrONO_2 is fully converted to the flux of Br_2 back to the atmosphere regardless of concurrent HBr deposition. Thus, as long as chemistry in the near-surface air favors the formation of HOBr and BrONO_2 over that of HBr , the atmospheric loading of bromine increases autocatalytically via bromine explosion over the FY sea ice.

On the MY sea ice, the supply of Br^- is assumed to be limited by the dry deposition of HBr from the atmosphere, because of substantial salinity decrease during summer melt in previous year(s) (Eicken et al., 2002). Also, the formation of open and refreezing leads as a fresh source of sea salt and/or brine is less likely to occur than in the FY sea ice that is more vulnerable to tensile force arising from surface wind drag and so forth (Richter-Menge and Jones, 1993; Sammonds et al., 1998; Kwok, 2006). The total dry deposition flux of HOBr and BrONO_2 , if it is not more than that of HBr , is fully converted to the Br_2 emission flux, whereas, if it exceeds that of HBr , the excess deposition of HOBr and BrONO_2 is converted to Br_2 at the 50% molar yield assuming as if BrCl were released instead of Br_2 to the atmosphere by consuming virtually inexhaustible Cl^- in the snowpack (Simpson et al., 2005). This formulation does not provide a net source of bromine to the atmosphere but recycles a part (between 50–100%) of inorganic bromine reservoirs into Br_2 . In reality, there may be some Br^- storage left over for later consumption to produce Br_2 . This possibility is ignored, but additional model runs are performed to explore if the MY sea ice can be as efficient at releasing Br_2 as the FY sea ice (Runs 6 to 8, see Table 3).

The snow-covered land surface is also assumed to emit Br_2 back to the atmosphere but with even less efficiency than the snowpack on the MY sea ice. The land snowpack is assumed to store no Cl^- and Br^- so that the Br_2 emission flux is determined by taking a smaller flux from either the dry deposition of HBr or the total dry deposition of HOBr and BrONO_2 . Consequently, a recycled fraction of bromine can vary from ~0% to 100%. At the horizontal scale of our model grid ($\approx 100 \text{ km} \times 100 \text{ km}$) it is not unreasonable to assume the absence of Cl^- for halogen re-activation in the snowpack

over land, since more than two orders of magnitude decrease in the snowpack Cl^- concentration has been observed within 150 km from the coastline in Alaska (Douglas and Sturm, 2004).

Bromine explosion and recycling processes cannot be initiated without a trigger. For this, more than a few mechanisms have been proposed, including the photolysis of CHBr_3 of biogenic origin (Tang and McConnell, 1996), the reactive uptake of ozone onto the ice/snow surface containing Br^- to release Br_2 (Oum et al., 1998) and the oxidation of Br^- by aqueous-phase OH radicals and other radical chain reaction products in the brine (Mozurkewich, 1995). Since quantitative details of these processes are too uncertain to be characterized across the Arctic, we choose to parameterize the trigger simply by associating ozone loss to the snow/ice surface via dry deposition with Br_2 emission back to the atmosphere. In this study, the surface resistance of ozone to the snow/ice surface is increased to 10^4 s m^{-1} (Helmig et al., 2007b) and thus its dry deposition velocity on the snowpack remains close to 0.01 cm s^{-1} under a variety of atmospheric conditions. In Runs 2 to 5 the trigger is placed on the FY sea ice only, whereas in Runs 6 to 8 the trigger is placed on the MY sea ice as well (Table 3). The trigger strength is assumed to be enhanced under sunlight. This is represented by changing the molar yield (Φ_1) of Br_2 against the amount of ozone lost via dry deposition with the solar zenith angle (SZA).

One of the simulation scenarios assumes that the dry deposition flux of ozone is converted to the Br_2 emission flux at $\Phi_1 = 10^{-3}$ regardless of SZA on the FY sea ice (Run 2, see Table 3). This is to represent Br_2 formation via reactive uptake of ozone onto frozen seawater in the dark (Oum et al., 1998). Theoretically, this leads to about 4 pmol mol^{-1} of Br_2 , within the range of Br_2 mixing ratios measured in the Arctic surface air during the polar night (Foster et al., 2001), in the boundary layer of 400 m depth in 5 days solely as a result of dry deposition of ozone at 40 nmol mol^{-1} . It turns out, however, that Φ_1 must be much larger for our model to simulate ODEs realistically as observed at stations in the high Arctic (see Sect. 3.1). We find that boundary-layer ODEs and BrO columns can be simulated quite reasonably by increasing Φ_1 to around

3-D modeling of Arctic boundary-layer bromine and ozone

K. Toyota et al.

[Title Page](#)[Abstract](#)[Introduction](#)[Conclusions](#)[References](#)[Tables](#)[Figures](#)[⏪](#)[⏩](#)[◀](#)[▶](#)[Back](#)[Close](#)[Full Screen / Esc](#)[Printer-friendly Version](#)[Interactive Discussion](#)

0.05 ~ 0.1 under sunlight. Thus, $\Phi = 0.075$ is assumed for $\text{SZA} \leq 85^\circ$ in our baseline scenario and most others (Runs 3 to 8, see Table 3). We will discuss implications of this fitted value later.

To map the concentrations of MY sea ice on a daily basis for the model, we use data retrieved from the QuikSCAT satellite by scatterometer signals at 13.4 GHz (K_u band) (Kwok, 2004). The FY sea ice concentrations are calculated by subtracting the MY sea ice concentrations from the total (sea, inland-water and glacier) ice concentrations available daily as part of Canadian Meteorological Centre (CMC) global data assimilation (Gauthier et al., 1999) with ice fractions for inland-water and glacier excluded by using land-use category data. CMC's sea ice analyses are largely based on Special Sensor Microwave/Imager (SSM/I) satellite data (Steffen et al., 1992). If grid-mean terrain height exceeds 50 m (hatched areas in Fig. 2), the fractional coverage of sea ice in a grid cell is ignored and snowpack is assumed to exist exclusively over land to avoid an unrealistic upward migration of reactive bromine in the stably stratified atmosphere.

As mentioned in the introduction, low temperature conditions are believed to be associated somehow with reactive halogen release in the polar boundary layer. In their observational study, Pöhler et al. (2010) concluded that snowpack in the Amundsen Gulf (in the Canadian Arctic) released reactive bromine to the atmosphere when surface air temperature was below -15°C and the rate of bromine release increased linearly with decreasing temperature down to -24°C . Based on this, we allow the release of Br_2 from the snowpack only where surface air temperature is at and below arbitrarily chosen "critical temperature" (T_c). We also vary T_c between -10°C and -20°C to study the sensitivity of simulated results on its choice (see Table 3). The snowpack is assumed not to release Br_2 but simply to act as a sink for atmospheric bromine where surface air temperature is above T_c . At present, the retrieval of MY sea ice from the QuikSCAT becomes unreliable at surface air temperatures above -10°C due to unmodeled changes in snow and ice properties (Kwok et al., 1999). Hence we do not explore the sensitivity of our model results on T_c beyond -10°C .

3-D modeling of Arctic boundary-layer bromine and ozone

K. Toyota et al.

[Title Page](#)[Abstract](#)[Introduction](#)[Conclusions](#)[References](#)[Tables](#)[Figures](#)[◀](#)[▶](#)[◀](#)[▶](#)[Back](#)[Close](#)[Full Screen / Esc](#)[Printer-friendly Version](#)[Interactive Discussion](#)

Emissions of aldehydes and nitrogen oxides from the snowpack can be of some importance for reactive halogen chemistry in the Arctic boundary layer (e.g., Piot and von Glasow, 2008). Our preliminary tests also showed that releasing HCHO from all the snow/ice-covered surface in the model at 4×10^9 molecule $\text{cm}^{-2} \text{s}^{-1}$, as employed by Michalowski et al. (2000) in their box model study, noticeably increased surface ozone mixing ratios simulated during ODEs at Alert and Barrow from below 1 nmol mol^{-1} to above 5 nmol mol^{-1} in many cases. At this point, however, spatial and temporal variations in the emissions of aldehydes and nitrogen oxides from the snowpack across the Arctic are quite uncertain. This issue is not pursued in the present study.

2.4 Simulation period and meteorological constraint

The GEM-AQ simulation is conducted in a series of 24-h free forecast segments from 06:00 UTC 15 March 2001 to 06:00 UTC 2 May 2001, for which 6-h trial fields of the CMC global analyses (Gauthier et al., 1999) are used for re-initializing meteorological and surface boundary conditions. Initial chemical and aerosol fields at 06:00 UTC 15 March 2001 are taken from an archive of global GEM-AQ simulation performed without bromine chemistry for the years 2001–2005 spun up from January 2000 (Kaminski et al., 2008). Initial mixing ratios of bromine species are set to zero but, as will be seen later, a spin-up period of about 15 days appears long enough for simulating reactive bromine production and ozone depletion in the Arctic boundary layer. Therefore model results are analyzed for the entire April in 2001.

Simulated surface meteorology is evaluated using automated meteorological observations available from across the Arctic during the simulated period (see Sect. S1 of the electronic Supplement). The model appears to capture synoptic disturbances as observed reasonably well at sites located within relatively smooth topography such as Barrow, whereas local effects are often pronounced but not well resolved by the model at sites located between steep subgrid-scale mountains such as Alert. In the latter case, evaluation of simulated tracer concentrations is compromised and short-term variability on a timescale of less than a day becomes rather meaningless.

3-D modeling of Arctic boundary-layer bromine and ozone

K. Toyota et al.

Title Page

Abstract

Introduction

Conclusions

References

Tables

Figures

◀

▶

◀

▶

Back

Close

Full Screen / Esc

Printer-friendly Version

Interactive Discussion



3 Results and discussion

Table 3 summarizes scenarios for model runs discussed in this study. Run 1 is to simulate a benchmark case without bromine chemistry, whereas Runs 2–8 are intended to test different scenarios for the surface source of bromine. Simulated results are evaluated first by using surface ozone and ozonesonde data obtained routinely at several Arctic sites. We will then look at day-to-day changes in simulated BrO column densities and compare them with data derived from satellite measurements.

3.1 Ground-level mixing ratios and vertical profiles of ozone

We began with tuning the molar yield (Φ_1) of Br₂ for a trigger reaction associated with the dry deposition of ozone, which is one of the most critical empirical parameters introduced in our model (see Sect. 2.3). For this, we used hourly data of surface ozone measurements at Alert, Barrow and Zeppelin where the link between spring-time ODEs and reactive bromine chemistry has been established by previous field campaigns (Simpson et al., 2007b). As indicated from statistical metrics (correlation coefficient, R ; mean bias, MB; and root mean squared error, RMSE) in Table 4, agreement between simulated and observed surface ozone mixing ratios at these three sites improves when simulated with an adjusted Φ_1 value ($= 0.075$) as compared to simulations without bromine chemistry (Run 1) and with a much smaller Φ_1 value ($= 0.001$, Run 2). At Alert and Barrow, the surface ozone mixing ratios simulated in Run 2 are almost the same as simulated in Run 1 and significantly larger than observed particularly during the ODEs. At Zeppelin, the values of MB and RMSE are apparently smaller when simulated without bromine chemistry (Run 1) than with bromine release from the snowpack by using the adjusted Φ_1 value (Runs 3–8), but, as discussed later, this is most likely caused by problems other than simulated bromine release. Note also that the value of R improves from 0.34 up to 0.58 at Zeppelin by introducing bromine release from the snowpack in the model.

3-D modeling of Arctic boundary-layer bromine and ozone

K. Toyota et al.

Title Page

Abstract

Introduction

Conclusions

References

Tables

Figures

◀

▶

◀

▶

Back

Close

Full Screen / Esc

Printer-friendly Version

Interactive Discussion



Figure 3a–c shows the time series of surface ozone mixing ratios simulated at Alert, Barrow and Zeppelin, respectively, in Run 1 (without bromine chemistry) and Run 4 ($T_c = -15^\circ\text{C}$ and FY sea ice is assumed more efficient at bromine release than MY sea ice) plotted along with hourly observational data from corresponding stations. Changes in simulated surface ozone mixing ratios across the nearest and eight neighboring grid cells are also indicated for each simulated time series, becoming important particularly at Alert because of inhomogeneous grid-mean terrain heights from 0 to 1215 m a.s.l. The site elevation of Alert GAW station (Fig. 2b), at which surface ozone data were obtained, is 210 m a.s.l., whereas the grid-mean terrain height is 565 m a.s.l. at the nearest grid cell of the model. Such a difference in height can be an important source of discrepancy between simulated and observed ozone mixing ratios in the stably stratified boundary layer prevailing in the high Arctic. The vertical extent of boundary-layer ODEs has been observed to vary between episodes from less than 100 m to as thick as 2000 m at and around Alert (Anlauf et al., 1994; Hopper et al., 1998; Bottenheim et al., 2002). Since one of the neighboring grid cells (location A' in Fig. 2b) does not contain mountains (but located entirely on the ocean mostly covered with MY sea ice), simulated ozone mixing ratios at the third lowest vertical level (~ 170 m a.s.l.) from this neighboring grid cell, along with those at the lowest vertical level from the nearest grid cell, are examined more closely than results from other neighboring grid cell. For the same reason, we look at simulated ozone mixing ratios for the nearest grid cell at the fourth lowest vertical level when compared with surface ozone data obtained at Zeppelin located on the crest of a mountain (474 m a.s.l.) unresolved by our model grid. Correlation coefficients between simulated and observed hourly ozone mixing ratios at Alert ($R = 0.79$ at the nearest grid cell and $R = 0.86$ at location A'), Barrow ($R = 0.68$) and Zeppelin ($R = 0.55$) are generally high for Run 4 with apparent improvement from Run 1 (Table 4), giving one of the grounds to believe that the model realistically represents reactive bromine release from the surface snowpack and subsequent ozone loss in the lower troposphere across the Arctic during the simulated period.

3-D modeling of Arctic boundary-layer bromine and ozone

K. Toyota et al.

Title Page

Abstract

Introduction

Conclusions

References

Tables

Figures

◀

▶

◀

▶

Back

Close

Full Screen / Esc

Printer-friendly Version

Interactive Discussion



3-D modeling of Arctic boundary-layer bromine and ozone

K. Toyota et al.

Title Page

Abstract

Introduction

Conclusions

References

Tables

Figures

◀

▶

◀

▶

Back

Close

Full Screen / Esc

Printer-friendly Version

Interactive Discussion



Ozonesonde data from across the Arctic provide additional insights into our simulations. In Fig. 6a–c, we compare observed and simulated ozone profiles between 0–6 km a.s.l. at Alert CFS, Resolute and Ny Ålesund, respectively. At Alert CFS (66 m a.s.l.), located only 6 km apart from Alert GAW station (see Fig. 2b), two out of the four ozone soundings in April 2001 were obtained during major ODEs lasting longer than 2 days. On 5 April, observed ozone mixing ratios were below 5 nmol mol⁻¹ from the ground up to 684 m a.s.l. and then gradually increased with altitude to reach 40 nmol mol⁻¹ at 2 km a.s.l. On 19 April, the vertical extent of the ozone-depleted layer was apparently smaller, with 12 nmol mol⁻¹ from the ground up to 183 m a.s.l. and then increased sharply to reach 36 nmol mol⁻¹ at 519 m a.s.l. These changes in observed ozone profiles are simulated quite reasonably with bromine chemistry included in the model, although the ozone mixing ratios are underpredicted notably between 1–3 km a.s.l. on 5 April. According to wind data from the ozonesonde and from the model, air mass origins on 5 April were vastly different between the ground level and above 1 m a.s.l., coming mainly from the north for the former and from the south for the latter (not shown). As discussed in Sect. 3.2, the model appears to have a tendency to overestimate reactive bromine release in Baffin Bay and narrows between Greenland and Ellesmere Island located to the south of Alert. At Resolute, located about 1100 km to the southwest of Alert, the observed profile on 7 April showed a near-complete ozone depletion ($O_3 < 1$ nmol mol⁻¹) below 400 m a.s.l. and recovered to 40 nmol mol⁻¹ at 1.2 km a.s.l. This profile is simulated quite reasonably by the model with bromine chemistry. Other two ozonesonde data from Resolute in April 2001 exhibited an indication of minor ODEs with an apparent decrease in boundary-layer ozone mixing ratios towards the ground level. Ozone profiles in these two cases are not simulated as well as the profile on 7 April, but the model with bromine chemistry does yield decreasing ozone mixing ratios towards the ground level in a more consistent manner than the model without bromine chemistry. Simulated ozone profiles at Ny Ålesund are also in fair agreement with observed profiles especially with regard to the vertical extent of boundary-layer air partially depleted in ozone; however, the model

often underpredicts ozone mixing ratios not only in the boundary layer but also in the free troposphere.

Changing T_c from -15°C to either -10°C (Run 3) or -20°C (Run 5) does not drastically impact simulated surface ozone mixing ratios at Alert, whereas the impacts are quite significant at Barrow and Zeppelin. Especially at Barrow, all the statistical metrics point to a better model performance with $T_c = -15^\circ\text{C}$ than with higher or lower T_c values (Table 4). Figure 4 shows the simulated time series of surface ozone mixing ratios for Runs 3 and 5 along with hourly observational data at Barrow. Obviously, the model starts to underrepresent the observed ODEs from mid April with $T_c = -20^\circ\text{C}$ (Run 5). Run 3, assuming $T_c = -10^\circ\text{C}$, captures the observed ODEs nearly as well as Run 4, while destroying ozone too much during some of the periods when surface ozone was observed to recover to 30 nmol mol^{-1} or higher at Barrow (e.g., 14–15 April, 21–23 April). These results are consistent with a recent observational study by Pöhler et al. (2010), in which they concluded that reactive bromine was released to the atmosphere when surface air temperature was lower than -15°C in the Amundsen Gulf.

At Zeppelin, the values of R suggest a better model performance in Runs 3 and 4 ($T_c = -10^\circ\text{C}$ or -15°C) than in Run 5 ($T_c = -20^\circ\text{C}$), but the trends of MB and RMSE values give a contradicting view (Table 4). As shown in Fig. 3c, the model underpredicts ozone mixing ratios almost all the time in Run 4 and, moreover, simulates a false occurrence of surface ozone dip during 14–16 April. Nonetheless, two episodes of relatively low ozone mixing ratios between $10 \sim 30\text{ nmol mol}^{-1}$ during 7–9 April and 21–23 April are reproduced fairly well. Simulated ozone profiles at Ny Ålesund, located in the same grid cell of the model as Zeppelin, point to a possibility that some of the underpredicted surface ozone mixing ratios at Zeppelin could be attributed to the low bias in background ozone levels above the boundary layer against observations (Fig. 6c). In addition, simulated sulfate aerosol concentrations are found to be overpredicted by a factor of 5–10 as compared to daily measurements at Zeppelin (see Sect. S2 of the electronic Supplement). Consequently, bromine chemistry around Zeppelin could be activated rather too intensively via heterogeneous reactions on the overpredicted

3-D modeling of Arctic boundary-layer bromine and ozone

K. Toyota et al.

[Title Page](#)[Abstract](#)[Introduction](#)[Conclusions](#)[References](#)[Tables](#)[Figures](#)[◀](#)[▶](#)[◀](#)[▶](#)[Back](#)[Close](#)[Full Screen / Esc](#)[Printer-friendly Version](#)[Interactive Discussion](#)

aerosol surface areas even if a source of bromine from the ice/snowpack surface was simulated reasonably in the model.

We have started our model runs by assuming that the snowpack on FY sea ice is more efficient at reactive bromine release than on MY sea ice as presumed by Simpson et al. (2007a). To explore the validity of this idea, sensitivity experiments are performed in which reactive bromine release on the MY sea ice is as efficient as on the FY sea ice (Runs 6 to 8, see Table 3). These model runs yield more widespread ODEs over the vast area of the Canadian side of the Arctic Ocean mainly covered with the MY sea ice as reflected in substantial changes in simulated ozone mixing ratios at the northern neighboring grid cell to Alert (location A', see Fig. 2b). If simply compared with ground-level ozone mixing ratios observed at Alert GAW station (Fig. 5) and with ozonesonde data from Alert CFS (Fig. 6a, particularly on 12 April 2001), the near-surface ozone mixing ratios at location A' are significantly underpredicted most of the time in Run 7 and therefore look unsatisfactory as compared to those simulated in Run 4 (Fig. 3a). The values of R for ozone mixing ratios simulated at location A' are apparently reduced for all the T_c ranges tested in Runs 6–8 ($R = 0.46 \sim 0.55$) from those obtained in Runs 3–5 ($R = 0.85 \sim 0.86$) and are even lower than that ($R = 0.78$) obtained in Run 1 without bromine chemistry (Table 4). But, according to previous field studies, ODEs on ice floes only 5 to 160 km apart from Alert CFS tend to be much more prolonged than those observed at nearby Alert stations (Hopper and Hart, 1994; Hopper et al., 1998; Morin et al., 2005). Surface snowpack on the MY sea ice near Alert can be substantially enriched in Br^- by late March (Ariya et al., 1999; Toom-Sauntry and Barrie, 2002). This could arise from the transport of gaseous and particulate bromine released from refrozen leads nearby and even from those rather distantly located if bromine deposited to the snowpack is re-emitted to the atmosphere successively (Simpson et al., 2005; Piot and von Glasow, 2008). Hence it is possible that ozone mixing ratios at location A' are actually simulated more realistically in Runs 6–8 (with no distinction between FY and MY sea ice surfaces for bromine release) than in Runs 3–5, which, however, cannot be assessed unambiguously owing to a lack of field ozone measurements on

3-D modeling of Arctic boundary-layer bromine and ozone

K. Toyota et al.

[Title Page](#)[Abstract](#)[Introduction](#)[Conclusions](#)[References](#)[Tables](#)[Figures](#)[⏪](#)[⏩](#)[◀](#)[▶](#)[Back](#)[Close](#)[Full Screen / Esc](#)[Printer-friendly Version](#)[Interactive Discussion](#)

ice floes near Alert during the simulated period. Surface ozone and ozonesonde data from other Arctic sites examined in the present study do not help very much, either, to draw a definitive conclusion about this issue.

At Summit, Greenland, simulated surface ozone mixing ratios are not very sensitive to bromine release from the snowpack on sea ice. The site (3238 m a.s.l.) is located above the typical height range where ozone profiles are influenced by bromine chemistry in our model at Alert, Resolute and Ny Ålesund (Fig. 6a–c). Relatively small MB and RMSE values for simulated surface ozone mixing ratios at Summit (Table 4) provide an assurance of model credibility for simulating background ozone levels around the site. The values of R , however, are generally low ($R < 0.3$) in all the model runs because of a poor capability of the model in reproducing a large daytime decrease in surface ozone mixing ratios (sometimes by more than 10 nmol mol^{-1}) particularly after 20 April 2001 (Fig. 3d). The reason for this discrepancy is not clear. Helmig et al. (2002) observed a daytime ozone decrease of similar magnitude occasionally at Summit during June 2000. A strong ozone sink in the local snowpack at Summit was also indicated by ozone measurements in the interstitial air (Helmig et al., 2007a). Recent field data indicates active bromine photochemistry occurring in the interstitial air of the snowpack as well as in the overlying ambient air at Summit in the summer (Dibb et al., 2010). On the other hand, Dibb et al. (2007) measured enhanced concentrations of dust mineral components in the surface snowpack at Summit particularly between 23–26 April 2001, originating most likely from Asian dust storms. As has been shown experimentally, certain dust minerals can promote the oxidation of halides into photolabile molecular halogens via heterogeneous surface reactions (Sadanaga et al., 2001; Anastasio and Mozurkewich, 2002).

Finally, it is worth noting results from another version of GEM-AQ by Zhao et al. (2008), which covered the same simulation period as ours. They assumed that airborne sea-salt particles originating from wind-abraded frost flowers provide a source of reactive bromine and chlorine species in the Arctic boundary layer. The locations of the frost flowers were determined based on the PFF data by Kaleschke et al. (2004). It

3-D modeling of Arctic boundary-layer bromine and ozone

K. Toyota et al.

Title Page

Abstract

Introduction

Conclusions

References

Tables

Figures

⏪

⏩

◀

▶

Back

Close

Full Screen / Esc

Printer-friendly Version

Interactive Discussion



appears that surface ozone mixing ratios at Alert, Barrow and Zeppelin were depleted much too frequently in the Zhao et al. (2008) model at least during April 2001 (see Fig. 3 in their paper), indicating either the irrelevance of frost flowers as a source of reactive bromine or inaccuracy in the PFF algorithm employed by Kaleschke et al. (2004).

3.2 Spatial and temporal evolutions of BrO columns

Space-borne measurements of BrO columns provide a useful means of evaluating our simulations particularly over sea ice where reactive bromine is actively released to the atmosphere. Here we use tropospheric BrO vertical column densities (VCDs) derived from a combination of total BrO columns measured by the Global Ozone Monitoring Experiment (GOME) instrument and BrO columns above the tropopause simulated by a stratospheric chemical transport model (Richter, 2006).

GOME is a UV/visible spectrometer on board the ERS-2 satellite. Slant column densities (SCDs) of atmospheric trace species are retrieved by applying a differential optical absorption algorithm to the measured spectra of sunlight scattered/reflected back from the earth's atmosphere in near-nadir ($\pm 32^\circ$) view geometry. For BrO, the spectral fitting window in the 345–359 nm wavelength region measured at 0.2 nm resolution is used (Richter et al., 2002). The BrO SCDs are then converted to VCDs by using air mass factors (AMFs) for an assumed stratospheric BrO profile with mixing ratios linearly increasing from 20 to 30 km and constant above 30 km (Richter et al., 1998). Data obtained where $\text{SZA} > 80^\circ$ are discarded here because retrieval sensitivity is skewed towards stratospheric BrO rather than tropospheric BrO. To obtain the tropospheric BrO columns, stratospheric BrO SCDs are subtracted from the total BrO SCDs by using output from the SLIMCAT middle-atmosphere chemical transport model (Chipperfield, 1999) at a horizontal resolution of $7.5^\circ \times 7.5^\circ$ driven by assimilated meteorology to address day-to-day changes in stratospheric dynamics and transport. The tropopause level is defined either by the potential temperature of 380 K or by the potential vorticity of 2 PVU (potential vorticity unit, $= 10^{-6} \text{ K m}^2 \text{ kg}^{-1} \text{ s}^{-1}$). The version of SLIMCAT used here has a total inorganic bromine (Br_y) loading in the stratosphere at

3-D modeling of Arctic boundary-layer bromine and ozone

K. Toyota et al.

Title Page

Abstract

Introduction

Conclusions

References

Tables

Figures

◀

▶

◀

▶

Back

Close

Full Screen / Esc

Printer-friendly Version

Interactive Discussion



the surface temperatures further. If bromine release from the snowpack is terminated at surface temperatures above -15°C , the model does not yield atmospheric bromine at the right time (and place) so that “BrO clouds” begin to lose a resemblance in their shape as compared to the GOME-SLIMCAT data (Fig. 7c). If $T_c = -20^{\circ}\text{C}$ is assumed, the “BrO clouds” in their maturity on 16–17 April and on 20 April are totally missed by the model (Fig. 7d). On the other side of the Arctic, a region that covers Hudson Bay and a southern part of Canadian Arctic Archipelago exhibited a frequent occurrence of “BrO clouds” during 15–22 April 2001. These events were also characterized by strong surface winds associated with synoptic disturbances, but surface temperatures did not increase so obviously as in the eastern Arctic cases described above because of air mass transport mainly from the north (Fig. 8a). Again, the “BrO clouds” do not emerge as seen in the GOME-SLIMCAT data particularly when $T_c = -20^{\circ}\text{C}$ is assumed in the model.

Figure 9a–f shows the scatter plots of GOME-SLIMCAT BrO VCDs versus BrO AVCDs simulated in Runs 3 to 8, respectively, during the entire April 2001 but sampled only to the north of 55°N and for $\text{SZA} \leq 80^{\circ}$. This confirms that the evolution of “BrO clouds” is best simulated with $T_c = -10^{\circ}\text{C}$, somewhat underrepresented if simulated with $T_c = -15^{\circ}\text{C}$ and significantly undermined with $T_c = -20^{\circ}\text{C}$. In addition, agreement between the model and the GOME-SLIMCAT data is slightly better when the FY sea ice is assumed to be more efficient at bromine release than the MY sea ice at least for $T_c = -15 \sim -10^{\circ}\text{C}$. We also note that, even in Run 3 which simulates the morphological evolutions of “BrO clouds” quite well, the values of BrO AVCDs are smaller than those of the GOME-SLIMCAT tropospheric BrO VCDs by more than a factor of two in many cases. This is puzzling because we ignore the effect of ice/water cloud cover to mask the “BrO clouds” underneath so that the BrO AVCDs from the model should be considered as an upper limit when looking at the events of increased bromine concentrations in the boundary layer. Over the bright snow/ice surface, a multiple-scattering of photons between the clouds and the surface would allow space-borne sensors to retain a considerable sensitivity to BrO below the cloud layer(s) but most likely to a

3-D modeling of Arctic boundary-layer bromine and ozone

K. Toyota et al.

[Title Page](#)[Abstract](#)[Introduction](#)[Conclusions](#)[References](#)[Tables](#)[Figures](#)[⏪](#)[⏩](#)[◀](#)[▶](#)[Back](#)[Close](#)[Full Screen / Esc](#)[Printer-friendly Version](#)[Interactive Discussion](#)

lesser extent than in the clear sky without the clouds (e.g., Vasilkov et al., 2010). Given that the boundary-layer ozone variations are simulated reasonably across the Arctic (see Sect. 3.1), it is not very promising to force the model results towards higher BrO concentrations by further adjusting the empirical parameters introduced for bromine release from the snowpack. There is an offset between the loss of ozone and the production of BrO in the boundary layer (e.g., Hausmann and Platt, 1994) so that increasing the rate of reactive bromine release does not necessarily lead to higher BrO concentrations in the model. We will return to this issue in Sect. 3.3.

Despite the general tendency of underpredicted BrO columns in the model, some regions of the Arctic, including Baffin Bay, often experience overpredicted BrO column values and/or false occurrence of simulated “BrO clouds” (see Fig. 7a–c). Flushing with meltwater is believed to be a primary mechanism to reduce salinity in sea ice and overlying snowpack in the summer (Holt and Digby, 1985; Eicken et al., 2002). In Barents Sea, Baffin Bay and Greenland Sea, melt-onset may occur as early as March to April with an interannual variability of more than a month (Drobot and Anderson, 2001a,b; Stroeve et al., 2006). Thus, in those areas, even on the FY sea ice the salinity may not be retained abundantly enough for the formation of “BrO clouds”. This appears to be linked to underpredicted ozone mixing ratios by the model between 1–3 km (with an indication of air mass transport from the south) as compared to the ozonesonde data from Alert CFS on 5 April 2001 (see Sect. 3.1 and Fig. 6a). Rather too frequent ODEs simulated at Zeppelin could also be attributed to the early melt-onset, but other probable reasons are already noted in Sect. 3.1 for the compromised capability of the model in simulating ODEs at Zeppelin.

Figure 8b shows surface ozone mixing ratios simulated in Run 4 at 12:00 UTC for each day between 15–22 April 2001. More than half of the ice-covered sea surface in the Arctic is simulated to be overlaid with surface air containing less than 20 nmol mol^{-1} of ozone. This is consistent with three-dimensional model studies by Zeng et al. (2003, 2006), in which they allocated the 3 to 5 day mean “tropospheric” BrO columns inferred from the GOME data to the lowest 300–400 m of the Arctic boundary layer for

3-D modeling of Arctic boundary-layer bromine and ozone

K. Toyota et al.

[Title Page](#)[Abstract](#)[Introduction](#)[Conclusions](#)[References](#)[Tables](#)[Figures](#)[⏪](#)[⏩](#)[◀](#)[▶](#)[Back](#)[Close](#)[Full Screen / Esc](#)[Printer-friendly Version](#)[Interactive Discussion](#)

simulating the ODEs. Our model shows that surface ozone is recovered to (near-) background levels ($>20 \text{ nmol mol}^{-1}$) where strong boundary-layer winds mediate a vertical and horizontal transport of ozone-rich air at synoptic scales as suggested previously from limited observations (Gong et al., 1997; Hopper et al., 1998; Strong et al., 2002; 5 Jacobi et al., 2010). High surface ozone levels and large wind speeds are both conducive to reactive bromine release in our model, because the bromine release is triggered via dry deposition of ozone at greater rates, bromine explosion is facilitated by a greater partitioning of HOBr (and BrONO₂ to a lesser extent) for a given amount of total inorganic bromine (Tang and McConnell, 1996), and dry deposition velocities of HOBr 10 and BrONO₂ increase substantially by a shear-induced turbulence in the otherwise statically stable boundary layer. The reasonable agreement in the simulated evolutions of “BrO clouds” with the GOME-SLIMCAT data indicates that, at least in April, a potential source of bromine to the atmosphere exists ubiquitously on the ice-covered ocean (particularly in areas covered with FY sea ice) across the Arctic and that the timing and 15 location of bromine release are controlled mainly by meteorological forcing on ozone transport and surface wind speed. The photochemical processing and movement of air mass containing “BrO clouds” will be smeared significantly if averaged over 3–5 days as was done by Zeng et al. (2003, 2006). This may explain why their correlation coefficients between simulated and observed surface ozone mixing ratios are somewhat 20 smaller ($R = 0.52 \sim 0.59$ at Alert and $R = 0.58 \sim 0.67$ at Barrow for the spring 2000) than our present results (see Table 4).

Bottenheim and Chan (2006) suggested that a majority of ODEs at Alert and Zepelin could have been initiated over sea ice several days upwind along trajectories across the central Arctic Ocean. Our model runs are not designed to reveal a link between specific “BrO clouds” and ODEs at downwind locations unambiguously. Such 25 a link, however, is indicated for some cases by looking at backward trajectories calculated by the CMC trajectory model using three-dimensional wind data from an operational GEM model (see Sect. S3 in the electronic Supplement for details). For instance, the arc-shaped “BrO cloud” matured off the coast of Siberia during 16–17 April 2001

3-D modeling of Arctic boundary-layer bromine and ozone

K. Toyota et al.

[Title Page](#)[Abstract](#)[Introduction](#)[Conclusions](#)[References](#)[Tables](#)[Figures](#)[⏪](#)[⏩](#)[◀](#)[▶](#)[Back](#)[Close](#)[Full Screen / Esc](#)[Printer-friendly Version](#)[Interactive Discussion](#)

appears to be an origin of the ODE at Alert on 20 April 2001 whereas the comma-shaped “BrO cloud” matured on 20 April 2001 appears to have carried air partially depleted in ozone to Zeppelin a few days later. Air mass depleted in ozone, once warmed adiabatically via vertical mixing while bromine chemistry is activated, can be cooled down by more than 10 K in a day or two as a result of infrared radiative cooling during the transport in the stable boundary layer over the snow/ice surface (Curry, 1983; Piot and von Glasow, 2008). Thus, the coincidence of ODEs and decreasing temperatures often observed at Arctic coastal sites such as Alert and Zeppelin (Bottenheim et al., 1990; Solberg et al., 1996; Tarasick and Bottenheim, 2002) may reflect a long transit time after ozone is destroyed at upwind locations rather than a measure of low temperature conditions required for activating bromine chemistry.

3.3 Additional BrO unaccounted for in the model

So far, we have examined the simulated BrO AVCDs without any offset applied when compared with the GOME-SLIMCAT tropospheric BrO VCDs. But it is probably reasonable to assume the presence of background BrO levels on the order of 1×10^{13} molecule cm^{-2} (or about $0.5 \sim 1$ pmol mol^{-1}) in the Arctic troposphere arising from sources neglected in our model runs such as the photodegradation of organic bromine and volatilization from sea-salt aerosols (Fitzenberger et al., 2000; Yang et al., 2005; Hendrick et al., 2007). Also, the BrO concentrations in the lowermost stratosphere are most likely underestimated by the SLIMCAT model used here because Chipperfield et al. (2005) did not account for very short-lived (VSL) organic bromine compounds such as CH_2Br_2 and CHBr_3 but represented the decomposition of organic source gases solely by $\text{CH}_3\text{Br} + \text{OH}/\text{hv}$. The “mean age of air”, time spent by air parcels after entering the stratosphere, is about 6 to 24 months in the Arctic lowermost stratosphere (e.g., Chipperfield, 2006), so that a fraction of CH_3Br already decomposed into inorganic bromine may change significantly with altitude (Dvortsov et al., 1999). More recent stratospheric chemical transport models (including the SLIMCAT model) assumed a contribution of VSL organic bromine compounds to the stratospheric Br_y

3-D modeling of Arctic boundary-layer bromine and ozone

K. Toyota et al.

Title Page

Abstract

Introduction

Conclusions

References

Tables

Figures

◀

▶

◀

▶

Back

Close

Full Screen / Esc

Printer-friendly Version

Interactive Discussion



loading in the range of $4 \sim 10 \text{ pmol mol}^{-1}$ to reconcile BrO levels with measurements from various platforms (e.g., Feng et al., 2007; Theys et al., 2009; Liang et al., 2010; Salawitch et al., 2005, 2010; Sioris et al., 2006; McLinden et al., 2010). There are also possible numerical issues with offline transport models and the use of analyzed winds (e.g., Schoeberl et al., 2003; Monge-Sanz et al., 2007). This may result in a significant underprediction of the mean age-of-air in the extra-tropical lower stratosphere and therefore degrade the simulation of Br_y profiles, resulting in lower predicted Br_y.

As shown in Fig. 10 by changes in dynamical tropopause levels (defined here by the 2 PVU surface) at 12:00 UTC for each day between 15–22 April 2001 simulated in the GEM model, the vertical displacement of the tropopause is strongly associated with synoptic disturbances controlling surface meteorology. Among the most striking is the collocation of lowered tropopause levels down to about 500 hPa encompassing from Canadian Arctic Archipelago to Hudson Bay with high BrO VCD values in the GOME-SLIMCAT data (Fig. 7a) during 20–22 April. Depending on the amount of stratospheric Br_y originating from VSL organic bromine compounds, such dynamical variability in the lowermost stratosphere could account for a significant part of variability in total BrO columns even in the springtime Arctic (Salawitch et al., 2010). For instance, a constant BrO mixing ratio at 3 pmol mol^{-1} between 200–500 hPa levels (which correspond to a range of variations in the dynamical tropopause level shown in Fig. 10) will translate to a BrO column at $1.9 \times 10^{13} \text{ molecule cm}^{-2}$. Together with the tropospheric BrO background, this could help reconcile the BrO columns simulated by the GEM-AQ model towards a better agreement with the GOME-SLIMCAT data. According to photochemical box model calculations (McLinden et al., 2010), about 50% of Br_y exists as BrO in the Arctic lowermost stratosphere in the middle of the day during this time of the year. Thus, 3 pmol mol^{-1} of extra BrO between 200–500 hPa is equivalent to adding 6 pmol mol^{-1} of stratospheric Br_y (either originating from VSL organic bromine compounds or accommodating numerical issues with tracer transport) to what was simulated by the SLIMCAT model from Chipperfield et al. (2005), well within the uncertainty range quoted above.

3-D modeling of Arctic boundary-layer bromine and ozone

K. Toyota et al.

[Title Page](#)[Abstract](#)[Introduction](#)[Conclusions](#)[References](#)[Tables](#)[Figures](#)[⏪](#)[⏩](#)[◀](#)[▶](#)[Back](#)[Close](#)[Full Screen / Esc](#)[Printer-friendly Version](#)[Interactive Discussion](#)

Here we show how BrO columns simulated by GEM-AQ (Run 3) can be corrected by adding extra BrO in the troposphere and/or in the lowermost stratosphere to reconcile with the GOME-SLIMCAT data. First, adding the extra 1 pmol mol^{-1} of background BrO in the entire troposphere (from the Earth surface up to the dynamical tropopause) removes an offset for the linear regression between GEM-AQ BrO AVCDs and GOME-SLIMCAT tropospheric BrO VCDs (Fig. 11a), but slightly reduces the correlation coefficient between the two quantities. Next, adding the extra $0.5 \text{ pmol mol}^{-1}$ of background BrO in the entire troposphere and 1 pmol mol^{-1} of BrO from the dynamical tropopause up to the 100 hPa level not only removes the offset for the linear regression but also improves the correlation coefficient from 0.64 to 0.68. Adding the extra $0.5 \text{ pmol mol}^{-1}$ of background BrO in the entire troposphere and 3 pmol mol^{-1} of BrO from the dynamical tropopause up to the 200 hPa level improves the correlation coefficient to 0.71 and, moreover, the slope of the linear regression is increased from 0.40 to 0.58. This reconciliation procedure works quite well over wide areas from middle to high latitudes of the northern hemisphere (see Figs. 12–13). But the conclusion that “BrO clouds” are boundary-layer phenomena still appears robust particularly over the eastern and central Arctic Ocean, because the horizontal structure of the vertical tropopause displacement (Fig. 10) does not necessarily agree with that of the enhanced BrO VCDs in the GOME-SLIMCAT data (Fig. 7a).

3.4 Role of temperature for gaseous bromine release from the condensed phase

There are more than a few reasons to believe that heterogeneous bromine activation is favored at lower temperatures: increasing concentrations of Br^- relative to Cl^- in the freezing brine particularly below -20°C due to the precipitation of $\text{NaCl} \cdot 2\text{H}_2\text{O}$ and $\text{MgCl}_2 \cdot 12\text{H}_2\text{O}$ (Koop et al., 2000; Morin et al., 2008); decreasing alkalinity via carbonate precipitation from freezing seawater as envisaged theoretically by Sander et al. (2006); and increasing capacity for the aerosol uptake of gaseous reactants (Piot and von Glasow, 2008). If liquid water content is as large as in boundary-layer clouds, it

3-D modeling of Arctic boundary-layer bromine and ozone

K. Toyota et al.

Title Page

Abstract

Introduction

Conclusions

References

Tables

Figures

◀

▶

◀

▶

Back

Close

Full Screen / Esc

Printer-friendly Version

Interactive Discussion



may rather deactivate bromine chemistry by an uptake of gaseous bromine species (Piot and von Glasow, 2008). The occurrence of mixed-phase clouds is very common in the Arctic boundary layer and their liquid water fraction increases notably with temperature (Shupe et al., 2006).

As shown above, our model evaluation based on the surface ozone, ozonesonde and satellite BrO column data indicates that reactive bromine release from the salty snow/ice surface should occur apparently at temperatures higher than -20°C . In our model runs it is assumed that the reactive uptake of O_3 , HOBr and BrONO_2 from the gas phase is responsible for reactive bromine release from the snowpack. To our knowledge, however, such reactions have not been characterized adequately by laboratory experiments at temperatures above -20°C . For the reactive uptake of HOBr onto frozen salt solutions, temperature ranges employed by previous laboratory experiments were limited between $-43 \sim -20^{\circ}\text{C}$ (Kirchner et al., 1997; Huff and Abbatt, 2002; Adams et al., 2002). Oum et al. (1998) conducted laboratory experiments of reactive ozone uptake on the frozen salt solution at temperatures between $-5 \sim -1^{\circ}\text{C}$ to find a significant bromine release to the gas phase, which cannot be compared in a quantitative manner with the HOBr uptake studies noted above. For the reactive uptake of BrONO_2 , experimental studies have not been conducted at temperature and substrate conditions pertinent to polar snowpack. Since the volume and chemical composition of the quasi-liquid layer at the frozen salt surface can change substantially with temperature (e.g., Abbatt, 2003), it is desirable to perform laboratory experiments consistently to explore if any changes occur in the reactive uptake coefficient and product yields of these heterogeneous reactions over wide temperature ranges for characterizing the chemistry of halogens in the polar boundary layer. In their recent laboratory experiment, N. Oldridge and J. Abbatt at University of Toronto found a significant increase in the reactive uptake coefficient of ozone onto frozen salt solution by raising temperature from -35°C to -15°C , indicating that substantial bromine release can indeed take place from the snowpack above -20°C .¹

¹Oldridge, N. and Abbatt, J.: Bromine Release from Ozone Heterogeneous Interactions 26236

3-D modeling of Arctic boundary-layer bromine and ozone

K. Toyota et al.

Title Page

Abstract

Introduction

Conclusions

References

Tables

Figures

◀

▶

◀

▶

Back

Close

Full Screen / Esc

Printer-friendly Version

Interactive Discussion



3.5 Is gaseous bromine released from the snowpack directly?

As discussed in Sect. 3.2, the timing and location of reactive bromine release to the atmosphere are strongly under the influence of meteorology changing time to time. Figure 14a shows the surface flux of Br_y integrated over 24 h on 20 April 2001 as simulated in Run 3. The net surface-to-air flux of Br_y is simulated to reach higher than $4 \times 10^{13} \text{ atom (Br) cm}^{-2} \text{ day}^{-1}$ in the eastern and central Arctic Ocean as well as in between Canadian Arctic Archipelago, contributing to the build up of “BrO clouds” located in these areas on the same day (Fig. 7a–b). The net surface-to-air Br_y flux is most likely overpredicted in Baffin Bay as noted before. The breakdown of contributing mechanisms, viz. the trigger of bromine explosion via dry deposition of ozone on the snow/ice surface of FY sea ice (Fig. 14b), Br_2 release via dry deposition of HOBr and BrONO_2 to the snow surface (Fig. 14e), the dry deposition of HBr, HOBr, BrONO_2 and Br_2 (Fig. 14f), and the wet deposition of HBr (Fig. 14c), points to a revealing fact about our simulation. Contrary to our original intention, the ozone trigger contributes primarily to a build up of atmospheric bromine in the model whereas the bromine explosion caused by HOBr and BrONO_2 is of secondary importance. Since the molar yield of Br_2 from the ozone trigger was obtained simply by a parameter tuning ($\Phi_1 = 0.075$, see Sect. 2.3), it is fair to consider that hidden processes are approximated fortuitously in our air-snowpack interaction scheme.

Sander et al. (2006) and Yang et al. (2008) envisaged that wind-abraded grains from the saline snowpack (drifting/blowing snow) serve as a major salinity source to the polar boundary layer and then lead to bromine explosion and ODEs. Such a surmise is consistent with ground-based optical measurements at Neumayer station, Antarctica by Frieß et al. (2004), which found enhanced overhead BrO columns often occurring with enhanced O_4 slant columns (as an indicator of aerosol multiple scattering). Jones et al. (2009) also found a compelling case where blowing snow was most likely involved with Frozen Salt Solutions: Evidence for Surface- and Bulk-Phase Reaction with Brine, to be submitted to J. Phys. Chem.

3-D modeling of Arctic boundary-layer bromine and ozone

K. Toyota et al.

Title Page

Abstract

Introduction

Conclusions

References

Tables

Figures

◀

▶

◀

▶

Back

Close

Full Screen / Esc

Printer-friendly Version

Interactive Discussion



3-D modeling of Arctic boundary-layer bromine and ozone

K. Toyota et al.

[Title Page](#)[Abstract](#)[Introduction](#)[Conclusions](#)[References](#)[Tables](#)[Figures](#)[⏪](#)[⏩](#)[◀](#)[▶](#)[Back](#)[Close](#)[Full Screen / Esc](#)[Printer-friendly Version](#)[Interactive Discussion](#)

in the occurrence of high BrO column and surface ozone depletion from ground-based observations at Halley station, Antarctica. Also in the Arctic, the occurrence of ODEs is sometimes accompanied by increased concentrations of sea-salt aerosols (e.g., Hop-
per and Hart, 1994). However, the concentrations of bromine in either gaseous or
particulate form are generally far in excess of what could be expected from sea-salt
composition (or sodium) in aerosols during the Arctic spring, indicating that a source
other than airborne sea-salt aerosols should account for most of the reactive bromine
in the air at least near coastal/island sites such as Alert, Barrow and Ny Ålesund (Berg
et al., 1983; Sturges and Barrie, 1988; Oltmans et al., 1989; Barrie et al., 1994; Lehrer
et al., 1997). Nonetheless, Yang et al. (2010) implemented an algorithm to simulate
the formation of blowing snow detached from saline snowpack on sea ice followed
by its sublimation to produce sea-salt aerosols in their three-dimensional tropospheric
chemical transport model with bromine chemistry. These authors concluded that the
amount of bromine originating from the wind-blown snow could be abundant enough
to account for the occurrence of “BrO clouds” in the springtime Arctic boundary layer.
Hence the inclusion of this process could have raised simulated BrO columns particu-
larly when windy in our model as well to give a further improvement in the correlation
and the slope of linear regression between simulated and measured BrO columns (see
Sect. 3.3).

On the other hand, if the bromine explosion takes place in the interstitial air of the
snowpack, it can produce a large amount of Br₂ while ozone imported from the over-
lying atmosphere is lost via gas-phase bromine chemistry. This process appears likely
to be happening because ozone destruction in the interstitial air, often enhanced by
sunlight, has been inferred from ozone measurements in the polar snowpack (Peter-
son and Honrath, 2001; Albert et al., 2002; Helmig et al., 2007a). Our air-snowpack
interaction scheme implicitly expresses such a linkage by relating the dry deposition
of ozone onto the snow surface to the release of Br₂ into the atmosphere. Theoretically,
the molar yield of Br₂ released to the atmosphere per mole of O₃ imported from
the ambient air and destroyed via gas-phase bromine chemistry in the interstitial air of

snowpack can be as high as 100%, if all the BrO radicals formed via Reaction (R1) undergo subsequent reactions only to form HOBr and BrONO₂ in the gas phase, then heterogeneously converted to Br₂ (Reactions R4–R5) and released to the atmosphere. This Br₂ molar yield can be even higher if there is a photochemical ozone production in the interstitial air as a result of NO₂ and/or HONO release via NO₃⁻ photolysis in the snowpack surface (e.g., Grannas et al., 2007), but it is more likely to be smaller than 100% considering a possibility of alternative reaction pathways such as the self-reaction of BrO (Reaction R2) to destroy ozone catalytically and the formation of HBr followed by its uptake to the ice surface before Br₂ is exported to the overlying ambient air. The pumping of air into and out of the snowpack is expected to increase with surface wind speed (e.g., Cunningham and Waddington, 1993), perhaps facilitating the Br₂ release from the snowpack if it is associated indeed with the ozone loss in the interstitial air.

At this point it is rather difficult to conclude which of the processes involving sea-salt particles originating from blowing snow and/or frost flowers, wind-pumping between the atmosphere and the snowpack or yet another unidentified mechanism plays a major role for the occurrence of “BrO clouds” across the Arctic.

4 Conclusions

Gas-phase and heterogeneous bromine chemistry and a simple scheme of air-snowpack chemical interactions were implemented in an online air-quality model, GEM-AQ, to simulate the production of reactive bromine species and the depletion of ozone in the springtime Arctic boundary layer. Model runs performed for April 2001 indicate that bromide (Br⁻) was retained ubiquitously in the snowpack on sea ice in the high Arctic and accessible from overlying ambient air to be released in the form of reactive gases such as Br₂. The timing and location of reactive bromine release appear to be controlled mainly by the horizontal and vertical transport of ozone-rich air mass, which facilitate the oxidation of Br⁻ in the snowpack directly and indirectly. Such transport events normally result from synoptic disturbances, which also break up the

3-D modeling of Arctic boundary-layer bromine and ozone

K. Toyota et al.

Title Page

Abstract

Introduction

Conclusions

References

Tables

Figures

◀

▶

◀

▶

Back

Close

Full Screen / Esc

Printer-friendly Version

Interactive Discussion



surface temperature inversion and raise temperatures at the air-snowpack interface. It was also shown that the snowpack is capable of actively releasing bromine at the air-snowpack interface temperatures of $-10 \sim -15^{\circ}\text{C}$ and possibly even higher. This, however, does not necessarily preclude the importance of lower temperature conditions, because some pre-conditioning processes such as brine expulsion on the top of refreezing leads may take place only below -20°C (Martin et al., 1996). Opening and refreezing of leads and resultant brine expulsion on the sea ice are probably the most active during the winter, but they still continue in the spring (Fett et al., 1994). The whole process starting from brine expulsion on sea ice and ending up with bromine release to the atmosphere may be occurring under vastly different temperature conditions.

Our air-snowpack interaction scheme yields a majority of atmospheric bromine input via Br_2 release empirically associated with a dry deposition of ozone on the snow/ice surface. This calls for scrutinizing the chemical and physical, presumably multiple-step, processes involved in the transformation of Br^- at the snow/ice surface into volatile gaseous bromine species. For instance, the pumping of ambient air into and out of the snowpack and the blowing/drifted snow lofted from the surface may both enhance the efficiency of heterogeneous reactions to activate bromine chemistry particularly under strong surface winds, which are also likely to carry ozone-rich air. The present model study also corroborates recent studies suggesting that transport processes associated with synoptic disturbances are critically involved in the occurrence of high tropospheric BrO column events both in the Arctic (Begoin et al., 2010) and in the Antarctic (Jones et al., 2010) as inferred from observed variability in ozone and BrO concentrations.

If the FY sea ice provides a ubiquitous source of reactive bromine as assumed in this study, the impacts of bromine chemistry on depleting ozone and mercury from the springtime Arctic boundary layer can be more extensive and intense in the future especially when sea ice totally disappears from the Arctic Ocean in the summer and thus consists of FY sea ice alone in the spring (Overland and Wang, 2007; Wang and Overland, 2009). But this assertion requires further scrutiny. Recently, Voulgarakis et al. (2009) simulated possible changes in ozone concentrations and oxidation capac-

3-D modeling of Arctic boundary-layer bromine and ozone

K. Toyota et al.

Title Page

Abstract

Introduction

Conclusions

References

Tables

Figures

◀

▶

◀

▶

Back

Close

Full Screen / Esc

Printer-friendly Version

Interactive Discussion



ity in the Arctic troposphere in response to the loss of sea ice from spring to summer by using a global chemical transport model with the effects of bromine chemistry and wind-blown snow. Their future scenarios and model configuration, however, did not include intricate details such as changes in physicochemical characters of saline ice/snow in response to warmer temperatures. Changes in meteorological conditions such as humidity, surface inversion and winds were not considered either. Our present capacity to address all of these issues is very limited. Given that our present results can be viewed as an indication of active bromine release nearly as well from the snowpack on MY sea ice in the middle of the spring, we also need to elucidate how bromine is recycled between the atmosphere and the snow/ice surface across the Arctic towards the summer.

Appendix A

Air mass factors applied to simulated BrO profiles

Vertically-resolved, or box, air mass factors (AMF_b) are calculated using the VECTOR (VECTor Orders-of-scattering Radiative transfer) model (McLinden et al., 2002, 2006). VECTOR accounts for the diurnal variation in BrO concentrations along the incoming solar beam, an effect that becomes important as twilight is approached, and was found to agree well with other models in an AMF-intercomparison study (Wagner et al., 2007). The AMF_b values are calculated by successively perturbing the BrO concentration in a layer and assessing its impact on the 350 nm nadir radiance.

A background atmosphere for 15 April at 65° N is employed. The profile is a combination of a photochemical box model-calculated stratospheric BrO profile (McLinden et al., 2000, 2010), and 1 pmol mol⁻¹ BrO in the troposphere. The use of a single BrO profile is justified as the AMFs are vertically resolved and hence independent of the profile shape, and also because BrO is optically thin. A background level of stratospheric sulfate aerosol at the optical depth of 0.02 and a tropospheric aerosol profile with a number density profile constant in altitude at the optical depth of 0.2 (Tomasi et al.,

3-D modeling of Arctic boundary-layer bromine and ozone

K. Toyota et al.

Title Page

Abstract

Introduction

Conclusions

References

Tables

Figures

◀

▶

◀

▶

Back

Close

Full Screen / Esc

Printer-friendly Version

Interactive Discussion



2007) are assumed. Based on this, a look-up table is generated as a function of altitude (1 km increments), surface albedo (0.2 increments), and solar zenith angle (13 between 0° and 90°, with the majority between 75° and 90°). A viewing zenith angle (θ_v) is set to 0° (pure nadir geometry). Multi-linear interpolation is used to determine the AMF_b for a given altitude (z), surface albedo (α , taken from broadband albedo for solar radiation in the GEM model), and solar zenith angle (θ_s).

Model apparent slant column densities (ASCs) are then calculated by vertically integrating the BrO number densities, weighted with the appropriate AMF_b. Finally, these ASCs are converted to adapted vertical column densities (AVCDs) by dividing them with geometric AMFs (AMF_g):

$$[\text{BrO AVCD}] = \frac{\int n_{\text{BrO}}(z) \text{AMF}_b(z, \alpha, \theta_s) dz}{\text{AMF}_g(\theta_v, \theta_s)} \quad (\text{A1})$$

where n_{BrO} is a vertical profile of simulated BrO number densities in molecule cm⁻³ and AMF_g is given by

$$\text{AMF}_g(\theta_v, \theta_s) = \frac{1}{\cos(\theta_v)} + \frac{1}{\cos(\theta_s)} \quad (\text{A2})$$

with $\theta_v = 0^\circ$ assumed again. This AMF_g approximates column-integrated AMFs for a purely stratospheric BrO profile used for the GOME-SLIMCAT tropospheric BrO VCD dataset within 15% for $\theta_s \leq 80^\circ$.

Supplementary material related to this article is available online at:

<http://www.atmos-chem-phys-discuss.net/10/26207/2010/acpd-10-26207-2010-supplement.pdf>

Acknowledgements. We thank A. Hussain and M. Neish for their assistance with computer programming for GEM-AQ, E. Chan of Environment Canada for providing surface ozone data from Alert, A. Platt of Environment Canada for the maintenance of meteorological equipments at Alert GAW station, and A.-G. Hjellbrekke of Norwegian Institute for Air Research

3-D modeling of Arctic boundary-layer bromine and ozone

K. Toyota et al.

Title Page

Abstract

Introduction

Conclusions

References

Tables

Figures

◀

▶

◀

▶

Back

Close

Full Screen / Esc

Printer-friendly Version

Interactive Discussion



for providing meteorological data from Zeppelin. We used surface ozone data for Barrow and Summit obtained electronically from NOAA/ESRL Global Monitoring Division (<http://www.esrl.noaa.gov/gmd/>) and for Zeppelin from the EMEP Chemical Coordinating Centre at Norwegian Institute of Air Research (<http://tarantula.nilu.no/projects/ccc/emepdata.html>).
5 Ozonesonde data were obtained from World Ozone and Ultraviolet Radiation Data Centre (<http://exp-studies.tor.ec.gc.ca/e/WOUDC.htm>). We also thank M. Samaali and J. Racine of the Canadian Meteorological Centre for assistance with back-trajectory analysis. KT is indebted to L. Kaleschke, T. L. Zhao, H. K. Roscoe, A. Dastoor, D. Durnford, T. Kikuchi, J. Inoue and J. Zhang for useful comments and discussion. This study was supported by Canadian Foundation for Climate and Atmospheric Sciences, Ontario Ministry of the Environment, Canada Foundation for Innovation, Ontario Innovation Trust, and Natural Sciences and Engineering Research Council of Canada. Analysis of the GOME BrO data was funded by the University of Bremen and the European Union THALOS project. The SLIMCAT modeling work at Leads was supported by the UK NCEO.

15 References

- Abbatt, J.: Interactions of atmospheric trace gases with ice surfaces: Adsorption and reaction, *Chem. Rev.*, 103, 4783–4800, 2003. 26236
- Adams, J. W., Holmes, N. S., and Crowley, J. N.: Uptake and reaction of HOBr on frozen and dry NaCl/NaBr surfaces between 253 and 233 K, *Atmos. Chem. Phys.*, 2, 79–91, doi:10.5194/acp-2-79-2002, 2002. 26212, 26213, 26236
- 20 Albert, M. R., Grannas, A. M., Bottenheim, J., Shepson, P. B., and Perron, F. E.: Processes and properties of snow-air transfer in the high Arctic with application to interstitial ozone at Alert, Canada, *Atmos. Environ.*, 36, 2779–2787, 2002. 26238
- Anastasio, C. and Mozurkewich, M.: Laboratory studies of bromide oxidation in the presence of ozone: Evidence for a glass-surface mediated reaction, *J. Atmos. Chem.*, 41, 135–162, 25 2002. 26227
- Anlauf, K. G., Mickle, R. E., and Trivett, N. B. A.: Measurement of ozone during Polar Sunrise Experiment 1992, *J. Geophys. Res.*, 99, 25345–25353, 1994. 26223
- Ariya, P. A., Hopper, J. F., and Harris, G. W.: C₂-C₇ hydrocarbon concentrations in Arctic snowpack interstitial air: Potential presence of active Br within the snowpack, *J. Atmos. Chem.*, 30 34, 55–64, 1999. 26226

3-D modeling of Arctic boundary-layer bromine and ozone

K. Toyota et al.

Title Page

Abstract

Introduction

Conclusions

References

Tables

Figures

◀

▶

◀

▶

Back

Close

Full Screen / Esc

Printer-friendly Version

Interactive Discussion



**3-D modeling of
Arctic boundary-layer
bromine and ozone**

K. Toyota et al.

[Title Page](#)[Abstract](#)[Introduction](#)[Conclusions](#)[References](#)[Tables](#)[Figures](#)[◀](#)[▶](#)[◀](#)[▶](#)[Back](#)[Close](#)[Full Screen / Esc](#)[Printer-friendly Version](#)[Interactive Discussion](#)

- Atkinson, R., Baulch, D. L., Cox, R. A., Crowley, J. N., Hampson, R. F., Hynes, R. G., Jenkin, M. E., Rossi, M. J., and Troe, J.: Evaluated kinetic and photochemical data for atmospheric chemistry: Volume III – reactions of inorganic halogens, *Atmos. Chem. Phys. Discuss.*, 6, 2281–2702, 2006a. 26258
- 5 Atkinson, R., Baulch, D. L., Cox, R. A., Crowley, J. N., Hampson, R. F., Hynes, R. G., Jenkin, M. E., Rossi, M. J., Troe, J., and IUPAC Subcommittee: Evaluated kinetic and photochemical data for atmospheric chemistry: Volume II - gas phase reactions of organic species, *Atmos. Chem. Phys.*, 6, 3625–4055, doi:10.5194/acp-6-3625-2006, 2006b. 26258
- 10 Atkinson, R., Baulch, D. L., Cox, R. A., Crowley, J. N., Hampson, R. F., Hynes, R. G., Jenkin, M. E., Rossi, M. J., and Troe, J.: Evaluated kinetic and photochemical data for atmospheric chemistry: Volume III - gas phase reactions of inorganic halogens, *Atmos. Chem. Phys.*, 7, 981–1191, doi:10.5194/acp-7-981-2007, 2007. 26258
- 15 Barrie, L. A., Bottenheim, J. W., Schnell, R. C., Crutzen, P. J., and Rasmussen, R. A.: Ozone destruction and photochemical reactions at polar sunrise in the lower Arctic troposphere, *Nature*, 334, 138–141, 1988. 26210, 26212
- Barrie, L. A., Li, S.-M., Toom, D. L., Landsberger, S., and Sturges, W.: Lower tropospheric measurements of halogens, nitrates, and sulphur oxides during Polar Sunrise Experiment 1992, *J. Geophys. Res.*, 99, 25453–25467, 1994. 26238
- 20 Bartlett, W. P. and Margerum, D. W.: Temperature dependencies of the Henry's law constant and the aqueous phase dissociation constant of bromine chloride, *Environ. Sci. Technol.*, 33, 3410–3414, 1999. 26259
- Begoin, M., Richter, A., Weber, M., Kaleschke, L., Tian-Kunze, X., Stohl, A., Theys, N., and Burrows, J. P.: Satellite observations of long range transport of a large BrO plume in the Arctic, *Atmos. Chem. Phys.*, 10, 6515–6526, doi:10.5194/acp-10-6515-2010, 2010. 26240
- 25 Berg, W., Sperry, P., Rahn, K., and Gladney, E.: Atmospheric bromine in the Arctic, *J. Geophys. Res.*, 88(C11), 6719–6736, 1983. 26238
- Bottenheim, J. W. and Chan, E.: A trajectory study into the origin of spring time Arctic boundary layer ozone depletion, *J. Geophys. Res.*, 111, D19301, doi:10.1029/2006JD007055, 2006. 26232
- 30 Bottenheim, J. W., Gallant, A. G., and Brice, K. A.: Measurements of NO_y species and O₃ at 82° N latitude, *Geophys. Res. Lett.*, 13, 113–116, 1986. 26210
- Bottenheim, J. W., Barrie, L. A., Atlas, E., Heidt, L. E., Niki, H., Rasmussen, R. A., and Shepson, P. B.: Depletion of lower tropospheric ozone during Arctic spring: The Polar Sunrise

**3-D modeling of
Arctic boundary-layer
bromine and ozone**

K. Toyota et al.

[Title Page](#)[Abstract](#)[Introduction](#)[Conclusions](#)[References](#)[Tables](#)[Figures](#)[◀](#)[▶](#)[◀](#)[▶](#)[Back](#)[Close](#)[Full Screen / Esc](#)[Printer-friendly Version](#)[Interactive Discussion](#)

Experiment 1988, *J. Geophys. Res.*, 95, 18555–18568, 1990. 26212, 26233

Bottenheim, J. W., Fuentes, J. D., Tarasick, D. W., and Anlauf, K. G.: Ozone in the Arctic lower troposphere during winter and spring 2000 (ALERT2000), *Atmos. Environ.*, 36, 2535–2544, 2002. 26210, 26223

5 Bottenheim, J. W., Netcheva, S., Morin, S., and Nghiem, S. V.: Ozone in the boundary layer air over the Arctic Ocean: measurements during the TARA transpolar drift 20062008, *Atmos. Chem. Phys.*, 9, 4545–4557, doi:10.5194/acp-9-4545-2009, 2009. 26210

Brimblecombe, P. and Clegg, S. L.: The solubility and behaviour of acid gases in the marine aerosol, *J. Atmos. Chem.*, 7, 1–18, 1988. 26259

10 Brimblecombe, P. and Clegg, S. L.: Erratum, 8, p. 95, 1989. 26259

Chance, K.: Analysis of BrO measurements from the Global Ozone Monitoring Experiment, *Geophys. Res. Lett.*, 25, 3335–3338, 1998. 26211

Chipperfield, M. P.: Multiannual simulations with a three-dimensional chemical transport model, *J. Geophys. Res.*, 104, 1781–1805, 1999. 26228

15 Chipperfield, M. P.: New version of the TOMCAT/SLIMCAT off-line chemical transport model: Intercomparison of stratospheric tracer experiments, *Q. J. Roy. Meteor. Soc.*, 132, 1179–1203, 2006. 26233

Chipperfield, M. P., Feng, W., and Rex, M.: Arctic ozone loss and climate sensitivity: Updated three-dimensional model study, *Geophys. Res. Lett.*, 32, L11813, doi:10.1029/2005GL022674, 2005. 26229, 26233, 26234

20 Côté, J., Gravel, S., Méhot, A., Patoine, A., Roch, M., and Staniforth, A.: The Operational CMC.MRB Global Environmental Multiscale (GEM) Model, Part I: Design Considerations and Formulation, *Mon. Weather Rev.*, 126, 1373–1395, 1998. 26215

Cunningham, J. and Waddington, E. D.: Air flow and dry deposition of non-sea salt sulfate in polar firn: Paleoclimatic implications, *Atmos. Environ.*, 27A, 2943–2956, 1993. 26239

25 Curry, J.: On the formation of continental polar air, *J. Atmos. Sci.*, 40, 2278–2292, 1983. 26233

DeMore, W. B., Sander, S. P., Golden, D. M., Hampson, R. F., Kurylo, M. J., Howard, C. J., Ravishankara, A. R., Kolb, C. E., and Molina, M. J.: Chemical Kinetics and Photochemical Data for Use in Stratospheric Modeling, Evaluation 12, JPL Publication 97-4, Jet Propulsion Laboratory, Pasadena, California, 1997. 26258

30 Dibb, J. E., Whitlow, S. I., and Arsenault, M.: Seasonal variations in the soluble ion content of snow at Summit, Greenland: Constraints from three years of daily surface snow samples, *Atmos. Environ.*, 41, 5007–5019, 2007. 26227

**3-D modeling of
Arctic boundary-layer
bromine and ozone**

K. Toyota et al.

Title Page

Abstract

Introduction

Conclusions

References

Tables

Figures

◀

▶

◀

▶

Back

Close

Full Screen / Esc

Printer-friendly Version

Interactive Discussion



- Dibb, J. E., Ziemba, L. D., Luxford, J., and Beckman, P.: Bromide and other ions in the snow, firn air, and atmospheric boundary layer at Summit during GSHOX, *Atmos. Chem. Phys.*, 10, 9931–9942, doi:10.5194/acp-10-9931-2010, 2010. 26227
- Douglas, T. A. and Sturm, M.: Arctic haze, mercury and the chemical composition of snow across northwestern Alaska, *Atmos. Environ.*, 38, 805–820, 2004. 26219
- 5 Drobot, S. D. and Anderson, M. R.: Comparison of interannual snowmelt-onset dates with atmospheric conditions, *Ann. Glaciol.*, 33, 79–84, 2001a. 26231
- Drobot, S. D. and Anderson, M. R.: An improved method for determining snowmelt onset dates over Arctic sea ice using scanning multichannel microwave radiometer and Special Sensor Microwave/Imager data, *J. Geophys. Res.*, 106, 24033–24049, 2001b. 26231
- 10 Dvortsov, V. L., Geller, M. A., Solomon, S., Schauffler, S. M., Atlas, E. L., and Blake, D. R.: Rethinking reactive halogen budgets in the midlatitude lower stratosphere, *Geophys. Res. Lett.*, 26(12), 1699–1702, 1999. 26233
- Eicken, H., Krouse, H. R., Kadko, D., and Perovich, D. K.: Tracer studies of pathways and rates of meltwater transport through Arctic summer sea ice, *J. Geophys. Res.*, 107(C10), 8046, doi:10.1029/2000JC000583, 2002. 26218, 26231
- 15 Fan, S.-M. and Jacob, D. J.: Surface ozone depletion in Arctic spring sustained by bromine reactions on aerosols, *Nature*, 359, 522–524, 1992. 26212
- Feng, W., Chipperfield, M. P., Dorf, M., Pfeilsticker, K., and Ricaud, P.: Mid-latitude ozone changes: studies with a 3-D CTM forced by ERA-40 analyses, *Atmos. Chem. Phys.*, 7, 2357–2369, doi:10.5194/acp-7-2357-2007, 2007. 26234
- 20 Fett, R. W., Burk, S. D., Thompson, W. T., and Kozo, T. L.: Environmental phenomena of the Beaufort Sea observed during the Leads Experiment, *B. Am. Meteorol. Soc.*, 75, 2131–2145, 1994. 26240
- 25 Fickert, S., Adams, J. W., and Crowley, J. N.: Activation of Br₂ and BrCl via uptake of HOBr onto aqueous salt solutions, *J. Geophys. Res.*, 104, 23719–23727, 1999. 26213
- Fitzenberger, R., Bosch, H., Camy-Peyret, C., Chipperfield, M. P., Harder, H., Platt, U., Sinnhuber, B.-M., Wagner, T., and Pfeilsticker, K.: First profile measurements of tropospheric BrO, *Geophys. Res. Lett.*, 27, 2921–2924, 2000. 26233
- 30 Foster, K. L., Plastridge, R. A., Bottenheim, J. W., Shepson, P. B., Finlayson-Pitts, B. J., and Spicer, C. W.: The role of Br₂ and BrCl in surface ozone destruction at polar sunrise, *Science*, 291, 471–474, 2001. 26213, 26219
- Frenzel, A., Scheer, V., Sikorski, R., George, C., Behnke, W., and Zetzsch, C.: Heterogeneous

**3-D modeling of
Arctic boundary-layer
bromine and ozone**

K. Toyota et al.

[Title Page](#)[Abstract](#)[Introduction](#)[Conclusions](#)[References](#)[Tables](#)[Figures](#)[◀](#)[▶](#)[◀](#)[▶](#)[Back](#)[Close](#)[Full Screen / Esc](#)[Printer-friendly Version](#)[Interactive Discussion](#)

interconversion reactions of BrNO_2 , ClNO_2 , Br_2 , and Cl_2 , *J. Phys. Chem. A*, 102, 1329–1337, 1998. 26259

Frieß, U., Wagner, T., Pundt, I., Pfeilsticker, K., and Platt, U.: Spectroscopic measurements of tropospheric iodine oxide at Neumayer Station, Antarctica, *Geophys. Res. Lett.*, 28, 1941–1944, 2001. 26211

Frieß, U., Hollwedel, J., Koönig-Langlo, G., Wagner, T., and Platt, U.: Dynamics and chemistry of tropospheric bromine explosion events in the Antarctic coastal region, *J. Geophys. Res.*, 109, D06305, doi:10.1029/2003JD004133, 2004. 26211, 26237

Gauthier, P., Charette, C., Fillion, L., Koclas, P., and Laroche, S.: Implementation of a 3-D assimilation system at the Canadian Meteorological Centre, Part I: The global analysis, *Atmos.-Ocean*, 37, 103–156, 1999. 26220, 26221

Gong, S. L., Walmsley, J. L., Barrie, L. A., and Hopper, J. F.: Mechanisms for surface ozone depletion and recovery during polar sunrise, *Atmos. Environ.*, 31, 969–981, 1997. 26232

Gong, S. L., Barrie, L. A., Blanchet, J. P., von Salzen, K., Lohmann, U., Lesins, G., Spacek, L., Zhang, L. M., Girard, E., Lin, H., Leaitch, R., Leighton, H., Chylek, P., and Huang, P.: Canadian Aerosol Module: A size-segregated simulation of atmospheric aerosol processes for climate and air quality models 1, Module development, *J. Geophys. Res.*, 108(D1), 4007, doi:10.1029/2001JD002002, 2003. 26216, 26258

Grannas, A. M., Jones, A. E., Dibb, J., Ammann, M., Anastasio, C., Beine, H. J., Bergin, M., Bottenheim, J., Boxe, C. S., Carver, G., Chen, G., Crawford, J. H., Dominé, F., Frey, M. M., Guzmán, M. I., Heard, D. E., Helmig, D., Hoffmann, M. R., Honrath, R. E., Huey, L. G., Hutterli, M., Jacobi, H. W., Klán, P., Lefer, B., McConnell, J., Plane, J., Sander, R., Savarino, J., Shepson, P. B., Simpson, W. R., Sodeau, J. R., von Glasow, R., Weller, R., Wolff, E. W., and Zhu, T.: An overview of snow photochemistry: evidence, mechanisms and impacts, *Atmos. Chem. Phys.*, 7, 4329–4373, doi:10.5194/acp-7-4329-2007, 2007. 26212, 26214, 26239

Hausmann, M. and Platt, U.: Spectroscopic measurement of bromine oxide and ozone in the high Arctic during Polar Sunrise Experiment 1992, *J. Geophys. Res.*, 99, 25399–25413, 1994. 26210, 26231

Helmig, D., Boulter, J., David, D., Birks, J. W., Cullen, N. J., Steffen, K., Johnson, B. J., and Oltmans, S. J.: Ozone and meteorological boundary-layer conditions at Summit, Greenland, during 3–21 June 2000, *Atmos. Environ.*, 36, 2595–2608, 2002. 26227

Helmig, D., Bocquet, F., Cohen, L., and Oltmans, S. J.: Ozone uptake to the polar snowpack at

**3-D modeling of
Arctic boundary-layer
bromine and ozone**

K. Toyota et al.

Title Page

Abstract

Introduction

Conclusions

References

Tables

Figures

◀

▶

◀

▶

Back

Close

Full Screen / Esc

Printer-friendly Version

Interactive Discussion



- Summit, Greenland, *Atmos. Environ.*, 41, 5061–5076, 2007a. 26227, 26238
- Helmig, D., Ganzeveld, L., Butler, T., and Oltmans, S. J.: The role of ozone atmosphere-snow gas exchange on polar, boundary-layer tropospheric ozone - a review and sensitivity analysis, *Atmos. Chem. Phys.*, 7, 15–30, doi:10.5194/acp-7-15-2007, 2007b. 26219
- 5 Hendrick, F., Van Roozendaal, M., Chipperfield, M. P., Dorf, M., Goutail, F., Yang, X., Fayt, C., Hermans, C., Pfeilsticker, K., Pommereau, J.-P., Pyle, J. A., Theys, N., and De Mazière, M.: Retrieval of stratospheric and tropospheric BrO profiles and columns using ground-based zenith-sky DOAS observations at Harestua, 60°N, *Atmos. Chem. Phys.*, 7, 4869–4885, doi:10.5194/acp-7-4869-2007, 2007. 26233
- 10 Holt, B. and Digby, S. A.: Processes and Imagery of First-Year Fast Sea Ice During the Melt Season, *J. Geophys. Res.*, 90, 5045–5062, 1985. 26231
- Hopper, J. F. and Hart, W.: Meteorological aspects of the 1992 Polar Sunrise Experiment, *J. Geophys. Res.*, 99, 25315–25328, 1994. 26226, 26238
- Hopper, J. F., Barrie, L. A., Silis, A., Hart, W., Gallant, A. J., and Dryfhout, H.: Ozone and meteorology during the 1994 Polar Sunrise Experiment, *J. Geophys. Res.*, 103, 1481–1492, 1998. 26210, 26223, 26226, 26232
- 15 Huff, A. K. and Abbatt, J. P. D.: Kinetics and product yields in the heterogeneous reactions of HOBr with ice surfaces containing NaBr and NaCl, *J. Phys. Chem. A*, 106(21), 5279–5287, 2002. 26236
- 20 IUPAC: IUPAC Subcommittee on Gas Kinetic Data Evaluation, Data Sheet oBrOx15, 3rd July 2005, <http://www.iupac-kinetic.ch.cam.ac.uk/>, 2005. 26258
- Jacobi, H.-W., Morin, S., and Bottenheim, J. W.: Observation of widespread depletion of ozone in the springtime boundary layer of the central Arctic linked to mesoscale synoptic conditions, *J. Geophys. Res.*, 115, D17302, doi:10.1029/2010JD013940, 2010. 26232
- 25 Jobson, B. T., Niki, H., Yokouchi, Y., Bottenheim, J., Hopper, F., and Leaitch, R.: Measurements of C₂-C₆ hydrocarbons during the Polar Sunrise 1992 Experiment: Evidence for Cl atom and Br atom chemistry, *J. Geophys. Res.*, 99, 25355–25368, 1994. 26212
- Jöckel, P., Tost, H., Pozzer, A., Brühl, C., Buchholz, J., Ganzeveld, L., Hoor, P., Kerkweg, A., Lawrence, M. G., Sander, R., Steil, B., Stiller, G., Tanarhte, M., Taraborrelli, D., van Aardenne, J., and Lelieveld, J.: The atmospheric chemistry general circulation model ECHAM5/MESSy1: consistent simulation of ozone from the surface to the mesosphere, *Atmos. Chem. Phys.*, 6, 5067–5104, doi:10.5194/acp-6-5067-2006, 2006. 26258
- 30 Jones, A. E., Anderson, P. S., Begoin, M., Brough, N., Hutterli, M. A., Marshall, G. J., Richter,

**3-D modeling of
Arctic boundary-layer
bromine and ozone**

K. Toyota et al.

Title Page

Abstract

Introduction

Conclusions

References

Tables

Figures

◀

▶

◀

▶

Back

Close

Full Screen / Esc

Printer-friendly Version

Interactive Discussion



A., Roscoe, H. K., and Wolff, E. W.: BrO, blizzards, and drivers of polar tropospheric ozone depletion events, *Atmos. Chem. Phys.*, 9, 4639–4652, doi:10.5194/acp-9-4639-2009, 2009. 26237

Jones, A. E., Anderson, P. S., Wolff, E. W., Roscoe, H. K., Marshall, G. J., Richter, A., Brough, N., and Colwell, S. R.: Vertical structure of Antarctic tropospheric ozone depletion events: characteristics and broader implications, *Atmos. Chem. Phys.*, 10, 7775–7794, doi:10.5194/acp-10-7775-2010, 2010. 26240

Kaleschke, L., Richter, A., Burrows, J., Afe, O., Heygster, G., Notholt, J., Rankin, A. M., Roscoe, H. K., Hollwedel, J., Wagner, T., and Jacobi, H. W.: Frost flowers on sea ice as a source of sea salt and their influence on tropospheric halogen chemistry, *Geophys. Res. Lett.*, 31, L16114, doi:10.1029/2004GL020655, 2004. 26213, 26214, 26227, 26228

Kaminski, J. W., Neary, L., Struzewska, J., McConnell, J. C., Lupu, A., Jarosz, J., Toyota, K., Gong, S. L., Côté, J., Liu, X., Chance, K., and Richter, A.: GEM-AQ, an on-line global multiscale chemical weather modelling system: model description and evaluation of gas phase chemistry processes, *Atmos. Chem. Phys.*, 8, 3255–3281, doi:10.5194/acp-8-3255-2008, 2008. 26215, 26216, 26221, 26258

Kirchner, U., Benter, T. H., and Schindler, R. N.: Experimental verification of gas phase bromine enrichment in reactions of HOBr with sea salt doped ice surfaces, *Ber. Bunsenges. Phys. Chem.*, 101, 975–977, 1997. 26236

Koop, T., Kapilashrami, A., Molina, L. T., and Molina, M. J.: Phase transitions of sea-salt/water mixtures at low temperatures: Implications for ozone chemistry in the polar marine boundary layer, *J. Geophys. Res.*, 105, 26393–26402, 2000. 26235

Kreher, K., Johnston, P. V., Wood, S. W., Nardi, B., and Platt, U.: Ground-based measurements of tropospheric and stratospheric BrO at Arrival Heights, Antarctica, *Geophys. Res. Lett.*, 24, 3021–3024, 1997. 26211

Kwok, R.: Annual cycles of multiyear sea ice coverage of the Arctic Ocean: 1999–2003, *J. Geophys. Res.*, 109, C11004, doi:10.1029/2004JC002238, 2004. 26214, 26220

Kwok, R.: Contrasts in sea ice deformation and production in the Arctic seasonal and perennial ice zones, *J. Geophys. Res.*, 111, C11S22, doi:10.1029/2005JC003246, 2006. 26218

Kwok, R., Cunningham, G. F., and Yueh, S.: Area balance of the Arctic Ocean perennial ice zone: October 1996 to April 1997, *J. Geophys. Res.*, 104, 25747–25759, 1999. 26220

Langner, J., Robertson, L., Persson, C., and Ullerstig, A.: Validation of the operational emergency response model at the Swedish Meteorological and Hydrological Institute using data

- from etex and the chernobyl accident, *Atmos. Environ.*, 32, 4325–4333, 1998. 26217
- Lax, E.: Taschenbuch für Chemiker und Physiker, Springer Verlag, Berlin, 1969. 26259
- Lehrer, E., Wagenbach, D., and Platt, U.: Aerosol chemical composition during tropospheric ozone depletion at Ny Ålesund/Svalbard, *Tellus*, 49B, 486–495, 1997. 26238
- 5 Lehrer, E., Hönninger, G., and Platt, U.: A one dimensional model study of the mechanism of halogen liberation and vertical transport in the polar troposphere, *Atmos. Chem. Phys.*, 4, 2427–2440, doi:10.5194/acp-4-2427-2004, 2004. 26211, 26217
- Li, S.-M., Yokouchi, Y., Barrie, L. A., Muthuramu, K., Shepson, P. B., Bottenheim, J. W., Sturges, W. T., and Landsberger, S.: Organic and inorganic bromine compounds and their composition in the Arctic troposphere during polar sunrise, *J. Geophys. Res.*, 99, 25415–25428, 1994. 26210
- 10 Liang, Q., Stolarski, R. S., Kawa, S. R., Nielsen, J. E., Douglass, A. R., Rodriguez, J. M., Blake, D. R., Atlas, E. L., and Ott, L. E.: Finding the missing stratospheric Br_y: a global modeling study of CHBr₃ and CH₂Br₂, *Atmos. Chem. Phys.*, 10, 2269–2286, doi:10.5194/acp-10-2269-2010, 2010. 26234
- 15 Light, B., Maykut, G. A., and Grenfell, T. C.: Effects of temperature on the microstructure of first-year Arctic sea ice, *J. Geophys. Res.*, 108(C2), 3051, doi:10.1029/2001JC000887, 2003. 26213
- Lupu, A., Kaminski, J. W., Neary, L., McConnell, J. C., Toyota, K., Rinsland, C. P., Bernath, P. F., Walker, K. A., Boone, C. D., Nagahama, Y., and Suzuki, K.: Hydrogen cyanide in the upper troposphere: GEM-AQ simulation and comparison with ACE-FTS observations, *Atmos. Chem. Phys.*, 9, 4301–4313, doi:10.5194/acp-9-4301-2009, 2009. 26215
- 20 Martin, S., Yu, Y., and Drucker, R.: The temperature dependence of frost flower growth on laboratory sea ice and the effect of the flowers on infrared observations of the surface, *J. Geophys. Res.*, 101(C5), 12111–12125, 1996. 26240
- McConnell, J. C., Henderson, G. S., Barrie, L., Bottenheim, J., Niki, H., Langford, C. H., and Templeton, E. M. J.: Photochemical bromine production implicated in Arctic boundary-layer ozone depletion, *Nature*, 355, 150–152, 1992. 26212
- 25 McLinden, C. A., Olsen, S., Hannegan, B., Wild, O., Prather, M. J., and Sundet, J.: Stratospheric ozone in 3-D models: A simple chemistry and the cross-tropopause flux, *J. Geophys. Res.*, 105, 14653–14665, 2000. 26241
- 30 McLinden, C. A., McConnell, J. C., Griffioen, E., and McElroy, C. T.: A vector radiative transfer model for the Odin/OSIRIS project, *Can. J. Phys.*, 80, 375–393, 2002. 26241

3-D modeling of Arctic boundary-layer bromine and ozone

K. Toyota et al.

[Title Page](#)[Abstract](#)[Introduction](#)[Conclusions](#)[References](#)[Tables](#)[Figures](#)[◀](#)[▶](#)[◀](#)[▶](#)[Back](#)[Close](#)[Full Screen / Esc](#)[Printer-friendly Version](#)[Interactive Discussion](#)

**3-D modeling of
Arctic boundary-layer
bromine and ozone**

K. Toyota et al.

Title Page

Abstract

Introduction

Conclusions

References

Tables

Figures

◀

▶

◀

▶

Back

Close

Full Screen / Esc

Printer-friendly Version

Interactive Discussion



- McLinden, C. A., Haley, C. S., and Sioris, C. E.: Diurnal effects in limb scatter observations, *J. Geophys. Res.*, 111, D14302, doi:10.1029/2005JD006628, 2006. 26241
- McLinden, C. A., Haley, C. S., Lloyd, N., Hendrick, F., Rozanov, A., Sinnhuber, B.-M., Goutail, F., Degenstein, D., Llewellyn, E., Sioris, C. E., Roozendael, M. V., Pommereau, J. P., Lotz, W., and Burrows, J. P.: Odin and OSIRIS observations of stratospheric BrO: Retrieval methodology, climatology, and inferred Bry, *J. Geophys. Res.*, 115, D15308, doi:10.1029/2009JD012488, 2010. 26234, 26241
- Michalowski, B. A., Francisco, J. S., Li, S. M., Barrie, L. A., Bottenheim, J. W., and Shepson, P. B.: A computer model study of multiphase chemistry in the Arctic boundary layer during polar sunrise, *J. Geophys. Res.*, 105, 15131–15145, 2000. 26211, 26212, 26221
- Monge-Sanz, B., Chipperfield, M. P., Simmons, A., and Uppala, S.: Mean age of air and transport in a CTM: Comparison of different ECMWF analyses, *Geophys. Res. Lett.*, 34, L04801, doi:10.1029/2006GL028515, 2007. 26234
- Morin, S., Hönninger, G., Staebler, R. M., and Bottenheim, J. W.: A high time resolution study of boundary layer ozone chemistry and dynamics over the Arctic Ocean near Alert, Nunavut, *Geophys. Res. Lett.*, 32, L08809, doi:10.1029/2004GL022098, 2005. 26226
- Morin, S., Marion, G. M., von Glasow, R., Voisin, D., Bouchez, J., and Savarino, J.: Precipitation of salts in freezing seawater and ozone depletion events: a status report, *Atmos. Chem. Phys.*, 8, 7317–7324, doi:10.5194/acp-8-7317-2008, 2008. 26213, 26235
- Mozurkewich, M.: Mechanisms for the release of halogens from sea-salt particles by free radical reactions, *J. Geophys. Res.*, 100, 14199–14207, 1995. 26219
- Murayama, S., Nakazawa, T., Tanaka, M., Aoki, S., and Kawaguchi, S.: Variations in tropospheric ozone concentration over Syowa Station, Antarctica, *Tellus*, 44B, 262–272, 1992. 26210
- Oltmans, S. J.: Surface ozone measurements in clean air, *J. Geophys. Res.*, 86, 1174–1180, 1981. 26210
- Oltmans, S. J., Schnell, R. C., Sheridan, P. J., Peterson, R. E., Li, S.-M., Winchester, J. W., Tans, P. P., Sturges, W. T., Kahl, J. D., and Barrie, L. A.: Seasonal surface ozone and filterable bromine relationship in the high Arctic, *Atmos. Environ.*, 23, 2431–2441, 1989. 26210, 26238
- O'Neill, N. T., Campanelli, M., Lupu, A., Thulasiraman, S., Reid, J. S., Aubé, M., Neary, L., Kaminski, J. W., and McConnell, J. C.: Evaluation of the GEM-AQ air quality model during the Québec smoke event of 2002: Analysis of extensive and intensive optical disparities, *Atmos. Environ.*, 40, 3737–3749, 2006. 26215

- Oum, K. W., Lakin, M. J., and Finlayson-Pitts, B. J.: Bromine activation in the troposphere by the dark reaction of O₃ with seawater ice, *Geophys. Res. Lett.*, 25, 3923–3926, 1998. 26219, 26236
- Overland, J. E. and Wang, M.: Future regional Arctic sea ice declines, *Geophys. Res. Lett.*, 34, L17705, doi:10.1029/2007GL030808, 2007. 26240
- Perovich, D. K. and Richter-Menge, J. A.: Surface characteristics of lead ice, *J. Geophys. Res.*, 99, 16341–16350, 1994. 26213
- Peterson, M. and Honrath, R.: Observations of rapid photochemical destruction of ozone in snowpack interstitial air, *Geophys. Res. Lett.*, 28, 511–514, 2001. 26238
- Piot, M. and von Glasow, R.: The potential importance of frost flowers, recycling on snow, and open leads for ozone depletion events, *Atmos. Chem. Phys.*, 8, 2437–2467, doi:10.5194/acp-8-2437-2008, 2008. 26221, 26226, 26233, 26235, 26236
- Pöhler, D., Vogel, L., Frieß, U., and Platt, U.: Observation of halogen species in the Amundsen Gulf, Arctic, by active long-path differential optical absorption spectroscopy, *Proc. Nat. Acad. Sci.*, 107, 6582–6587, doi:10.1073/pnas.0912231107, 2010. 26220, 26225
- Ramacher, B., Rudolph, J., and Koppmann, R.: Hydrocarbon measurements during tropospheric ozone depletion events: Evidence for halogen atom chemistry, *J. Geophys. Res.*, 104, 3633–3653, 1999. 26212
- Rankin, A. M., Wolff, E. W., and Martin, S.: Frost flowers: Implications for tropospheric chemistry and ice core interpretation, *J. Geophys. Res.*, 107(D23), 4683, doi:10.1029/2002JD002492, 2002. 26213
- Richter, A.: GOME tropospheric BrO columns Version 1, available at: http://www.iup.uni-bremen.de/doas/gome.bro_data.htm, 2006. 26228
- Richter, A., Wittrock, F., Eisinger, M., and Burrows, J. P.: GOME observations of tropospheric BrO in northern hemispheric spring and summer 1997, *Geophys. Res. Lett.*, 25, 2683–2686, 1998. 26211, 26228
- Richter, A., Wittrock, F., Ladstätter-Weißmayer, A., and Burrows, J.: GOME measurements of stratospheric and tropospheric BrO, *Adv. Space Res.*, 29, 1667–1672, 2002. 26228
- Richter-Menge, J. A. and Jones, K. F.: The tensile strength of first-year sea ice, *J. Glaciol.*, 39, 609–618, 1993. 26218
- Sadanaga, Y., Hirokawa, J., and Akimoto, H.: Formation of molecular chlorine in dark condition: Heterogeneous reaction of ozone with sea salt in the presence of ferric ion, *Geophys. Res. Lett.*, 28(23), 4433–4436, 2001. 26227

3-D modeling of Arctic boundary-layer bromine and ozone

K. Toyota et al.

[Title Page](#)[Abstract](#)[Introduction](#)[Conclusions](#)[References](#)[Tables](#)[Figures](#)[◀](#)[▶](#)[◀](#)[▶](#)[Back](#)[Close](#)[Full Screen / Esc](#)[Printer-friendly Version](#)[Interactive Discussion](#)

5 Saiz-Lopez, A., Mahajan, A. S., Salmon, R. A., Bauguitte, S. J.-B., Jones, A. E., Roscoe, H. K., and Plane, J. M. C.: Boundary layer halogens in coastal Antarctica, *Science*, 317, 348–351, 2007. 26211

10 Salawitch, R. J., Weisenstein, D. K., Kovalenko, L. J., Sioris, C. E., Wennberg, P. O., Chance, K., Ko, M. K. W., and McLinden, C. A.: Sensitivity of ozone to bromine in the lower stratosphere, *Geophys. Res. Lett.*, 32, L05811, doi:10.1029/2004GL021504, 2005. 26234

15 Salawitch, R. J., Canty, T., Kurosu, T., Chance, K., Liang, Q., da Silva, A., Pawson, S., Nielsen, J. E., Rodriguez, J., Bhartia, P., Liu, X., Huey, L., Liao, J., Stickel, R., Simpson, W., Donohue, D., Weinheimer, A., Flocke, F., Knapp, D., Montzka, D., Neuman, J., Nowak, J., Ryerson, T., Oltmans, S., Blake, D., Atlas, E. L., Kinnison, D., Tilmes, S., Pan, L., Hendrick, F., Rozendael, M. V., Kreher, K., Johnston, P., Gao, R. S., Johnson, B., Bui, T., Chen, G., Pierce, R. B., Crawford, J. H., and Jacob, D. J.: A New Interpretation of Total Column BrO during Arctic Spring, *Geophys. Res. Lett.*, 37, L21805, doi:10.1029/2010GL043798, 2010. 26234

20 Sammonds, P. R., Murrell, S. A. F., and Rist, M. A.: Fracture of multiyear sea ice, *J. Geophys. Res.*, 103, 21795–21815, 1998. 26218

Sander, R. and Morin, S.: Introducing the bromide/alkalinity ratio for a follow-up discussion on “Precipitation of salts in freezing seawater and ozone depletion events: a status report”, by Morin et al., published in *Atmos. Chem. Phys.*, 8, 7317–7324, 2008, *Atmos. Chem. Phys.*, 10, 7655–7658, doi:10.5194/acp-10-7655-2010, 2010. 26213

25 Sander, R., Kerkweg, A., Jöckel, P., and Lelieveld, J.: Technical note: The new comprehensive atmospheric chemistry module MECCA, *Atmos. Chem. Phys.*, 5, 445–450, doi:10.5194/acp-5-445-2005, 2005. 26216

Sander, R., Burrows, J., and Kaleschke, L.: Carbonate precipitation in brine - a potential trigger for tropospheric ozone depletion events, *Atmos. Chem. Phys.*, 6, 4653–4658, doi:10.5194/acp-6-4653-2006, 2006. 26213, 26235, 26237

30 Schoeberl, M. R., Douglass, A. R., Zhu, Z., and Pawson, S.: A comparison of the lower stratospheric age spectra derived from a general circulation model and two data assimilation systems, *J. Geophys. Res.*, 108(D3), 4113, doi:10.1029/2002JD002652, 2003. 26234

Schönhardt, A., Richter, A., Wittrock, F., Kirk, H., Oetjen, H., Roscoe, H. K., and Burrows, J. P.: Observations of iodine monoxide columns from satellite, *Atmos. Chem. Phys.*, 8, 637–653, doi:10.5194/acp-8-637-2008, 2008. 26211

Shupe, M. D., Matrosov, S. Y., and Uttal, T.: Arctic mixed-phase cloud properties derived from

3-D modeling of Arctic boundary-layer bromine and ozone

K. Toyota et al.

Title Page

Abstract

Introduction

Conclusions

References

Tables

Figures

◀

▶

◀

▶

Back

Close

Full Screen / Esc

Printer-friendly Version

Interactive Discussion



**3-D modeling of
Arctic boundary-layer
bromine and ozone**

K. Toyota et al.

Title Page

Abstract

Introduction

Conclusions

References

Tables

Figures

◀

▶

◀

▶

Back

Close

Full Screen / Esc

Printer-friendly Version

Interactive Discussion



surface-based sensors at SHEBA, *J. Atmos. Sci.*, **63**, 697–711, 2006. 26236

Simpson, W. R., Alvarez-Aviles, L., Douglas, T. A., Sturm, M., and Domine, F.: Halogens in the coastal snow pack near Barrow, Alaska: Evidence for active bromine air-snow chemistry during springtime, *Geophys. Res. Lett.*, **32**, L04811, doi:10.1029/2004GL021748, 2005. 26212, 26218, 26226

Simpson, W. R., Carlson, D., Hönninger, G., Douglas, T. A., Sturm, M., Perovich, D., and Platt, U.: First-year sea-ice contact predicts bromine monoxide (BrO) levels at Barrow, Alaska better than potential frost flower contact, *Atmos. Chem. Phys.*, **7**, 621–627, doi:10.5194/acp-7-621-2007, 2007a. 26214, 26217, 26226

Simpson, W. R., von Glasow, R., Riedel, K., Anderson, P., Ariya, P., Bottenheim, J., Burrows, J., Carpenter, L., Frieß, U., Goodsite, M. E., Heard, D., Hutterli, M., Jacobi, H.-W., Kaleschke, L., Neff, B., Plane, J., Platt, U., Richter, A., Roscoe, H., Sander, R., Shepson, P., Sodeau, J., Steffen, A., Wagner, T., and Wolff, E.: Halogens and their role in polar boundary-layer ozone depletion, *Atmos. Chem. Phys.*, **7**, 4375–4418, 2007b. 26214, 26222

Sioris, C. E., Kovalenko, L. J., McLinden, C. A., Salawitch, R. J., Roozendael, M. V., Goutail, F., Dorf, M., Pfeilsticker, K., Chance, K., von Savigny, C., Liu, X., Kurosu, T. P., Pomereau, J.-P., Bösch, H., and Frerick, J.: Latitudinal and vertical distribution of bromine monoxide in the lower stratosphere from Scanning Imaging Absorption Spectrometer for Atmospheric Chartography limb scattering measurements, *J. Geophys. Res.*, **111**, D14301, doi:10.1029/2005JD006479, 2006. 26234

Solberg, S., Schmidbauer, N., Semb, A., Stordal, F., and Hov, O.: Boundary-layer ozone depletion as seen in the Norwegian Arctic in spring, *J. Atmos. Chem.*, **23**, 301–332, 1996. 26210, 26212, 26233

Spicer, C. W., Plastridge, R. A., Foster, K. L., Finlayson-Pitts, B. J., Bottenheim, J. W., Grannas, A. M., and Shepson, P. B.: Molecular halogens before and during ozone depletion events in the Arctic at polar sunrise: concentrations and sources, *Atmos. Environ.*, **36**, 2721–2731, 2002. 26213

Steffen, A., Douglas, T., Amyot, M., Ariya, P., Aspmo, K., Berg, T., Bottenheim, J., Brooks, S., Cobbett, F., Dastoor, A., Dommergue, A., Ebinghaus, R., Ferrari, C., Gardfeldt, K., Goodsite, M. E., Lean, D., Poulain, A. J., Scherz, C., Skov, H., Sommar, J., and Temme, C.: A synthesis of atmospheric mercury depletion event chemistry in the atmosphere and snow, *Atmos. Chem. Phys.*, **8**, 1445–1482, doi:10.5194/acp-8-1445-2008, 2008. 26214

Steffen, K. and DeMaria, T.: Surface energy fluxes of Arctic winter sea ice in Barrow Strait, *J.*

3-D modeling of Arctic boundary-layer bromine and ozone

K. Toyota et al.

[Title Page](#)
[Abstract](#)
[Introduction](#)
[Conclusions](#)
[References](#)
[Tables](#)
[Figures](#)
[Back](#)
[Close](#)
[Full Screen / Esc](#)
[Printer-friendly Version](#)
[Interactive Discussion](#)


Appl. Meteorol., 35, 2067–2079, 1996. 26213

Steffen, K., Key, J., Cavalieri, D. J., Comiso, J., Gloersen, P., Germain, K. S., and Rubinstein, I.: The Estimation of Geophysical Parameters Using Passive Microwave Algorithms, in: Microwave Remote Sensing of Sea Ice, edited by: Carsey, F. D., vol. 68, chap. 10, Geophysical Monograph, American Geophysical Union, 1992. 26220

Stockwell, W. R. and Lurmann, F. W.: Intercomparison of the ADOM and RADM Gas-Phase Chemistry Mechanisms, Report prepared for the Electric Power Research Institute, Electric Power Research Institute, Palo Alto, California, 1989. 26216

Stroeve, J., Markus, T., Meier, W. N., and Miller, J.: Recent changes in the Arctic melt season, Ann. Glaciol., 44, 367–374, 2006. 26231

Strong, C., Fuentes, J. D., Davis, R. E., and Bottenheim, J. W.: Thermodynamic attributes of Arctic boundary layer ozone depletion, Atmos. Environ., 36, 2641–2652, 2002. 26232

Struzewska, J. and Kaminski, J. W.: Formation and transport of photooxidants over Europe during the July 2006 heat wave - observations and GEM-AQ model simulations, Atmos. Chem. Phys., 8, 721–736, doi:10.5194/acp-8-721-2008, 2008. 26215

Sturges, W. T. and Barrie, L. A.: Chlorine, bromine and iodine in arctic aerosols, Atmos. Environ., 22, 1179–1194, 1988. 26238

Tang, T. and McConnell, J. C.: Autocatalytic release of bromine from Arctic snow pack during polar sunrise, Geophys. Res. Lett., 23, 2633–2636, 1996. 26211, 26219, 26232

Tarasick, D. W. and Bottenheim, J. W.: Surface ozone depletion episodes in the Arctic and Antarctic from historical ozonesonde records, Atmos. Chem. Phys., 2, 197–205, doi:10.5194/acp-2-197-2002, 2002. 26210, 26233

Theys, N., Van Roozendael, M., Errera, Q., Hendrick, F., Daerden, F., Chabrillat, S., Dorf, M., Pfeilsticker, K., Rozanov, A., Lotz, W., Burrows, J. P., Lambert, J.-C., Goutail, F., Roscoe, H. K., and De Mazière, M.: A global stratospheric bromine monoxide climatology based on the BASCOE chemical transport model, Atmos. Chem. Phys., 9, 831–848, doi:10.5194/acp-9-831-2009, 2009. 26234

Tomasi, C., Vitale, V., Lupi, A., Carmine, C. D., Campanelli, M., Herber, A., Treffeisen, R., Stone, R. S., Andrews, E., Sharma, S., Radionov, V., von Hoyningen-Huene, W., Stebel, K., Hansen, G. H., Myhre, C. L., Wehrli, C., Aaltonen, V., Lihavainen, H., Virkkula, A., Hillamo, R., Ström, J., Toledano, C., Cachorro, V. E., Ortiz, P., de Frutos, A. M., Blindheim, S., Frioud, M., Gausa, M., Zielinski, T., Petelski, T., and Yamanouchi, T.: Aerosols in polar regions: A historical overview based on optical depth and in situ observations, J. Geophys. Res., 112,

3-D modeling of Arctic boundary-layer bromine and ozone

K. Toyota et al.

[Title Page](#)
[Abstract](#)
[Introduction](#)
[Conclusions](#)
[References](#)
[Tables](#)
[Figures](#)
[Back](#)
[Close](#)
[Full Screen / Esc](#)
[Printer-friendly Version](#)
[Interactive Discussion](#)


D16205, doi:10.1029/2007JD008432, 2007. 26241

Toom-Sauntry, D. and Barrie, L. A.: Chemical composition of snowfall in the high Arctic: 1990–1994, *Atmos. Environ.*, 36, 2683–2693, 2002. 26226

Toyota, K., Kanaya, Y., Takahashi, M., and Akimoto, H.: A box model study on photochemical interactions between VOCs and reactive halogen species in the marine boundary layer, *Atmos. Chem. Phys.*, 4, 1961–1987, doi:10.5194/acp-4-1961-2004, 2004. 26216

Tuckermann, M., Ackermann, R., Göltz, C., Lorenzen-schmidt, H., Senne, T., Stutz, J., Trost, B., Unold, W., and Platt, U.: DOAS-observation of halogen radical-catalysed arctic boundary layer ozone destruction during the ARCTOC-campaigns 1995 and 1996 in Ny-Ålesund, Spitsbergen, *Tellus*, 49B, 533–555, 1997. 26210, 26211

Vasilkov, A. P., Joiner, J., Haffner, D., Bhartia, P. K., and Spurr, R. J. D.: What do satellite backscatter ultraviolet and visible spectrometers see over snow and ice? A study of clouds and ozone using the A-train, *Atmos. Meas. Tech.*, 3, 619–629, doi:10.5194/amt-3-619-2010, 2010. 26231

Vogt, R., Crutzen, P. J., and Sander, R.: A mechanism for halogen release from sea-salt aerosol in the remote marine boundary layer, *Nature*, 383, 327–330, 1996. 26216

Voulgarakis, A., Yang, X., and Pyle, J. A.: How different would tropospheric oxidation be over an ice-free Arctic?, *Geophys. Res. Lett.*, 36, L23807, doi:10.1029/2009GL040541, 2009. 26240

Wagner, T. and Platt, U.: Satellite mapping of enhanced BrO concentrations in the troposphere, *Nature*, 395, 486–490, 1998. 26211

Wagner, T., Leue, C., Wenig, M., Pfeilsticker, K., and Platt, U.: Spatial and temporal distribution of enhanced boundary layer BrO concentrations measured by the GOME instrument aboard ERS-2, *J. Geophys. Res.*, 106, 24225–24235, 2001. 26211

Wagner, T., Burrows, J. P., Deutschmann, T., Dix, B., von Friedeburg, C., Frieß, U., Hendrick, F., Heue, K.-P., Irie, H., Iwabuchi, H., Kanaya, Y., Keller, J., McLinden, C. A., Oetjen, H., Palazzi, E., Petritoli, A., Platt, U., Postlyakov, O., Pukite, J., Richter, A., van Roozendaal, M., Rozanov, A., Rozanov, V., Sinreich, R., Sanghavi, S., and Wittrock, F.: Comparison of box-air-mass-factors and radiances for Multiple-Axis Differential Optical Absorption Spectroscopy (MAX-DOAS) geometries calculated from different UV/visible radiative transfer models, *Atmos. Chem. Phys.*, 7, 1809–1833, doi:10.5194/acp-7-1809-2007, 2007. 26241

Wang, M. and Overland, J. E.: A sea ice free summer Arctic within 30 years?, *Geophys. Res. Lett.*, 36, L07502, doi:10.1029/2009GL037820, 2009. 26240

Wennberg, P.: Atmospheric chemistry – Bromine explosion, *Nature*, 397, 299–301, 1999.

26211

Wesely, M. L.: Parameterization of surface resistances to gaseous dry deposition in regional-scale numerical models, *Atmos. Environ.*, 23, 1293–1304, 1989. 26217

Wessel, S., Aoki, S., Winkler, P., Weller, R., Herber, A., Gernandt, H., and Schrems, O.: Tropospheric ozone depletion in polar regions. A comparison of observations in the Arctic and Antarctic, *Tellus*, 50B, 34–50, 1998. 26210

Yang, X., Cox, R. A., Warwick, N. J., Pyle, J. A., Carver, G. D., O'Connor, F. M., and Savage, N. H.: Tropospheric bromine chemistry and its impacts on ozone: A model study, *J. Geophys. Res.*, 110, D23311, doi:10.1029/2005JD006244, 2005. 26216, 26233

Yang, X., Pyle, J. A., and Cox, R. A.: Sea salt aerosol production and bromine release: Role of snow on sea ice, *Geophys. Res. Lett.*, 35, L16815, doi:10.1029/2008GL034536, 2008. 26214, 26237

Yang, X., Pyle, J. A., Cox, R. A., Theys, N., and Van Roozendael, M.: Snow-sourced bromine and its implications for polar tropospheric ozone, *Atmos. Chem. Phys.*, 10, 7763–7773, doi:10.5194/acp-10-7763-2010, 2010. 26214, 26238

Yurganov, L. N.: Surface layer ozone above the Weddell Sea during the Antarctic spring, *Antarctic Science*, 2, 169–174, 1990. 26210

Zeng, T., Wang, Y., Chance, K., Browell, E. V., Ridley, B. A., and Atlas, E. L.: Widespread persistent near-surface ozone depletion at northern high latitude in spring, *Geophys. Res. Lett.*, 30(24), 2298, doi:10.1029/2003GL018587, 2003. 26231, 26232

Zeng, T., Wang, Y., Chance, K., Blake, N., Blake, D., and Ridley, B.: Halogen-driven low-altitude O₃ and hydrocarbon losses in spring at northern high latitudes, *J. Geophys. Res.*, 111, D17313, doi:10.1029/2005JD006706, 2006. 26231, 26232

Zhang, L., Moran, M. D., Makar, P. A., Brook, J. R., and Gong, S.: Modelling gaseous dry deposition in AURAMS: a unified regional air-quality modelling system, *Atmos. Environ.*, 36, 537–560, 2002. 26217

Zhao, T. L., Gong, S., Bottenheim, J. W., McConnell, J. C., Sander, R., Kaleschke, L., Richter, A., Kerkweg, A., Toyota, K., and Barrie, L. A.: A three-dimensional model study on the production of BrO and Arctic boundary layer ozone depletion, *J. Geophys. Res.*, 113, D24304, doi:10.1029/2008JD01063, 2008. 26216, 26217, 26227, 26228

ACPD

10, 26207–26278, 2010

3-D modeling of Arctic boundary-layer bromine and ozone

K. Toyota et al.

Title Page

Abstract

Introduction

Conclusions

References

Tables

Figures

◀

▶

◀

▶

Back

Close

Full Screen / Esc

Printer-friendly Version

Interactive Discussion



Table 1. Gas-phase, heterogeneous, and photolysis reactions of bromine species added to GEM-AQ for this study.^{a,b}

No.	Reaction	Rate constant ^c	Reference
Gas-phase reactions			
G119	$\text{Br} + \text{O}_3 \rightarrow \text{BrO} (+\text{O}_2)$	$k = 1.7 \times 10^{-11} \exp(-800/T)$	1
G120	$\text{BrO} + \text{BrO} \rightarrow \text{Br} + \text{Br} (+\text{O}_2)$	$k = 2.7 \times 10^{-12}$	1
G121	$\text{BrO} + \text{BrO} \rightarrow \text{Br}_2 (+\text{O}_2)$	$k = 2.9 \times 10^{-14} \exp(840/T)$	1
G122	$\text{BrO} + \text{NO} \rightarrow \text{Br} + \text{NO}_2$	$k = 8.7 \times 10^{-12} \exp(260/T)$	1
G123	$\text{Br} + \text{HO}_2 \rightarrow \text{HBr} (+\text{O}_2)$	$k = 7.7 \times 10^{-12} \exp(-450/T)$	1
G124	$\text{Br} + \text{HCHO} \xrightarrow{\text{O}_3} \text{HBr} + \text{CO} + \text{HO}_2$	$k = 7.7 \times 10^{-12} \exp(-580/T)$	2
G125	$\text{Br} + \text{ALD}_2 \xrightarrow{\text{O}_3} \text{HBr} + \text{MCO}_3$	$k = 1.8 \times 10^{-11} \exp(-460/T)$	2
G126	$\text{OH} + \text{HBr} \rightarrow \text{Br} (+\text{H}_2\text{O})$	$k = 5.5 \times 10^{-12} \exp(205/T)$	3
G127	$\text{BrO} + \text{NO}_2 + \text{M} \rightarrow \text{BrONO}_2 + \text{M}$	$k_0 = 4.7 \times 10^{-31} (T/300)^{-3.1} [\text{M}]$ $k_\infty = 1.8 \times 10^{-11}, F_2 = 0.4$	1 ^d
G128	$\text{BrO} + \text{HO}_2 \rightarrow \text{HOBr} (+\text{O}_2)$	$k = 4.5 \times 10^{-12} \exp(500/T)$	1
G129	$\text{BrO} + \text{MO}_2 \xrightarrow{\text{O}_3} \text{HCHO} + 0.75 \times \text{HOBr} + 0.25 \times \text{Br} + 0.25 \times \text{HO}_2$	$k = 5.7 \times 10^{-12}$	4
Heterogeneous reactions			
G130	$\text{HOBr} \rightarrow 0.5 \times \text{Br}_2$	$\gamma = 0.1$	see Note ^e
G131	$\text{BrONO}_2 \rightarrow \text{HOBr} + \text{HNO}_3$	$\gamma = 0.1$	see Note ^e
G132	$\text{HBr} \rightarrow 0.5 \times \text{Br}_2$	$\gamma = 0.1$	see Note ^e
Photolysis reactions			
P20	$\text{BrO} + h\nu \rightarrow \text{Br} + \text{O}$		see Note ^f
P21	$\text{Br}_2 + h\nu \rightarrow \text{Br} + \text{Br}$		see Note ^f
P22	$\text{HOBr} + h\nu \rightarrow \text{Br} + \text{OH}$		see Note ^f
P23	$\text{BrONO}_2 + h\nu \rightarrow \text{Br} + \text{NO}_3$		see Note ^f

References: 1 Atkinson et al. (2007); 2 Atkinson et al. (2006b); 3 Atkinson et al. (2006a); 4 IUPAC (2005).

^a See Kaminski et al. (2008) for the list of other reactions included in GEM-AQ.

^b $\text{ALD}_2 = \text{CH}_3\text{CHO}$ and higher aldehydes, assumed to react as CH_3CHO , $\text{MCO}_3 = \text{CH}_3\text{CO}_3$, and $\text{MO}_2 = \text{CH}_3\text{O}_2$.

^c The unit of rate constants for gas-phase reactions (G119–129) is $\text{cm}^3 \text{ molecule}^{-1} \text{ s}^{-1}$.

^d See Atkinson et al. (2007) for the formulation detail of the pseudo-second-order rate constant of termolecular reaction (G127).

^e Heterogeneous reactions on the aerosol surface whose first-order rate constants (in s^{-1}) are calculated by the modified Fuchs-Sutugin equation as described in Gong et al. (2003) using an estimated reaction probability ($\gamma = 0.1$). However, the HBr loss rate via Reaction (G132) and the sum of the HOBr loss rate via Reaction (G130) and the BrONO_2 loss rate via Reaction (G131) are diagnosed before the numerical integration of chemical tendency equations and, if the former is larger than the latter (i.e., $k_{\text{G132}}[\text{HBr}] > k_{\text{G130}}[\text{HOBr}] + k_{\text{G131}}[\text{BrONO}_2]$), the rate constant for Reaction (G132) is scaled down so as to equalize the two diagnosed quantities.

^f Absorption cross sections and quantum yields as adopted by the MESSy/JVAL submodel (Jöckel et al., 2006) and based largely on DeMore et al. (1997).

3-D modeling of Arctic boundary-layer bromine and ozone

K. Toyota et al.

Title Page

Abstract

Introduction

Conclusions

References

Tables

Figures

◀

▶

◀

▶

Back

Close

Full Screen / Esc

Printer-friendly Version

Interactive Discussion



3-D modeling of Arctic boundary-layer bromine and ozone

K. Toyota et al.

Table 2. Effective Henry's law constants (H^*) at neutral pH and oxidative reactivity parameters (f_0) for calculating the dry deposition velocities of inorganic bromine species except on the snow/ice covered surface.

Species	H^* [M atm ⁻¹]	f_0
Br ₂	8×10^{-1} (see ^a)	1
HOBr	6×10^3 (see ^b)	1
BrONO ₂	2×10^{16} (see ^c)	1
HBr	2×10^{16} (see ^d)	0

^a Taken from Bartlett and Margerum (1999).

^b Taken from Frenzel et al. (1998).

^c Assumed to be the same as for HBr.

^d Calculated based on Brimblecombe and Clegg (1988, 1989) and Lax (1969).

[Title Page](#)
[Abstract](#)
[Introduction](#)
[Conclusions](#)
[References](#)
[Tables](#)
[Figures](#)
[Back](#)
[Close](#)
[Full Screen / Esc](#)
[Printer-friendly Version](#)
[Interactive Discussion](#)


3-D modeling of Arctic boundary-layer bromine and ozone

K. Toyota et al.

Table 3. Description of model runs: “critical temperature” (T_c) at and below which the snowpack acquires a capability of releasing Br_2 (2nd column), locations where the trigger via dry deposition of O_3 and the bromine explosion via dry deposition of HOBr and BrONO_2 are assumed to occur (3rd column), and the molar yield (Φ_1) of Br_2 for the “trigger reaction” associated with the dry deposition of O_3 (4th column).

Run #	T_c	Trigger and bromine explosion	Φ_1
1		No bromine release from the snowpack, viz. no bromine chemistry in the atmosphere	
2	-10°C	On FY sea ice only	0.001 regardless of SZA
3	-10°C	On FY sea ice only	0.001 for $\text{SZA} > 85^\circ$, 0.075 for $\text{SZA} \leq 85^\circ$
4	-15°C	On FY sea ice only	0.001 for $\text{SZA} > 85^\circ$, 0.075 for $\text{SZA} \leq 85^\circ$
5	-20°C	On FY sea ice only	0.001 for $\text{SZA} > 85^\circ$, 0.075 for $\text{SZA} \leq 85^\circ$
6	-10°C	On both FY & MY sea ice	0.001 for $\text{SZA} > 85^\circ$, 0.075 for $\text{SZA} \leq 85^\circ$
7	-15°C	On both FY & MY sea ice	0.001 for $\text{SZA} > 85^\circ$, 0.075 for $\text{SZA} \leq 85^\circ$
8	-20°C	On both FY & MY sea ice	0.001 for $\text{SZA} > 85^\circ$, 0.075 for $\text{SZA} \leq 85^\circ$

[Title Page](#)
[Abstract](#)
[Introduction](#)
[Conclusions](#)
[References](#)
[Tables](#)
[Figures](#)
[Back](#)
[Close](#)
[Full Screen / Esc](#)
[Printer-friendly Version](#)
[Interactive Discussion](#)


3-D modeling of Arctic boundary-layer bromine and ozone

K. Toyota et al.

Table 4. Correlation coefficients (R), mean biases (MB, in nmol mol^{-1}) and root mean squared errors (RMSE, in nmol mol^{-1}) of simulated surface ozone mixing ratios against hourly data of in-situ measurements at Alert, Barrow, Zeppelin and Summit for all the model runs. The simulated values are taken from the lowest model level, except for Zeppelin where the fourth vertical model level (~ 470 m a.s.l.) is chosen to best match the altitude of the station. The nearest grid cell for Alert has a grid-mean terrain height of 565 m a.s.l., which is significantly higher than the actual height of surface ozone measurements (210 m a.s.l.), so that the statistical metrics are also presented for the third lowest vertical level (~ 170 m a.s.l.) at one of the neighboring grid cells (location A' in Fig.2b).

Run #	Alert						Barrow			Zeppelin			Summit		
	Nearest Grid Cell			Location A'			Nearest Grid Cell			Nearest Grid Cell			Nearest Grid Cell		
	R	MB	RMSE	R	MB	RMSE	R	MB	RMSE	R	MB	RMSE	R	MB	RMSE
1	0.66	+16.0	21.8	0.78	+13.7	19.5	0.56	+21.0	24.0	0.34	+3.0	8.2	0.22	+2.4	7.9
2	0.68	+15.4	21.2	0.77	+12.9	18.7	0.62	+19.6	22.5	0.35	+2.3	7.9	0.23	+2.3	7.8
3	0.78	+3.5	11.1	0.85	-3.9	10.0	0.66	-6.3	11.5	0.58	-10.5	12.7	0.27	+0.1	7.7
4	0.79	+4.9	11.6	0.86	-2.8	9.3	0.68	-1.8	9.6	0.55	-9.1	11.7	0.26	+0.8	7.6
5	0.76	+7.5	13.5	0.86	+0.1	8.9	0.57	+5.1	11.9	0.45	-6.4	9.9	0.25	+1.3	7.7
6	0.75	-0.3	11.3	0.55	-14.0	20.6	0.67	-9.0	13.0	0.55	-14.0	16.0	0.27	-0.2	7.7
7	0.74	+0.7	11.4	0.46	-14.7	22.1	0.64	-4.9	11.1	0.50	-13.0	15.5	0.26	+0.5	7.6
8	0.73	+2.4	11.8	0.46	-13.8	21.7	0.53	+1.2	11.3	0.41	-10.6	13.8	0.25	+1.1	7.7

[Title Page](#)
[Abstract](#)
[Introduction](#)
[Conclusions](#)
[References](#)
[Tables](#)
[Figures](#)
[Back](#)
[Close](#)
[Full Screen / Esc](#)
[Printer-friendly Version](#)
[Interactive Discussion](#)


3-D modeling of
Arctic boundary-layer
bromine and ozone

K. Toyota et al.

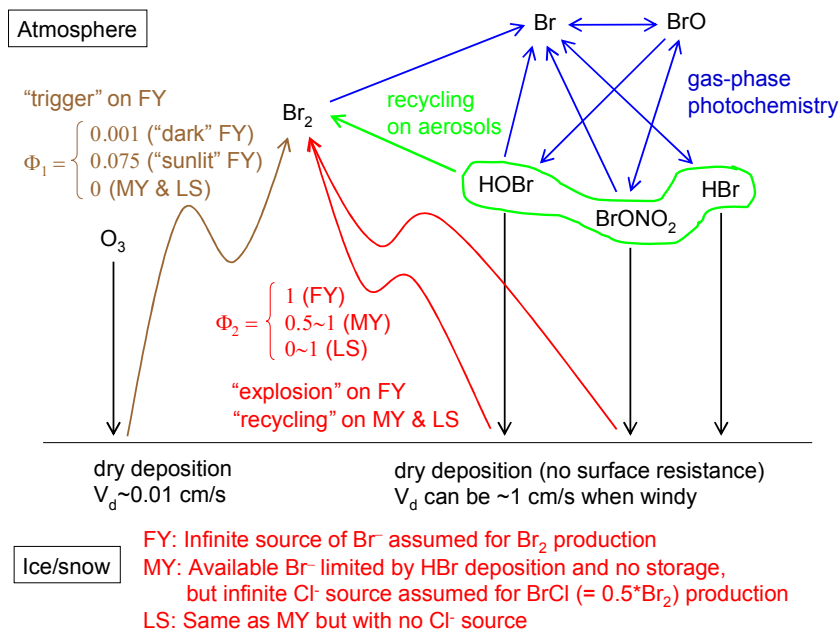


Fig. 1. A schematic of the scenario for bromine chemistry in the atmosphere and air-ice/snow interactions of reactive bromine species in the present simulations. FY, MY and LS denote snowpack on FY sea ice, MY sea ice and land surface, respectively. The molar yields (Φ_1 and Φ_2) of Br_2 from the dry deposition of O_3 , HOBr and BrONO_2 shown here are for the model runs 3–5 and changed somewhat in other runs (see Table 3).

Title Page

Abstract

Introduction

Conclusions

References

Tables

Figures

◀

▶

◀

▶

Back

Close

Full Screen / Esc

Printer-friendly Version

Interactive Discussion



3-D modeling of Arctic boundary-layer bromine and ozone

K. Toyota et al.

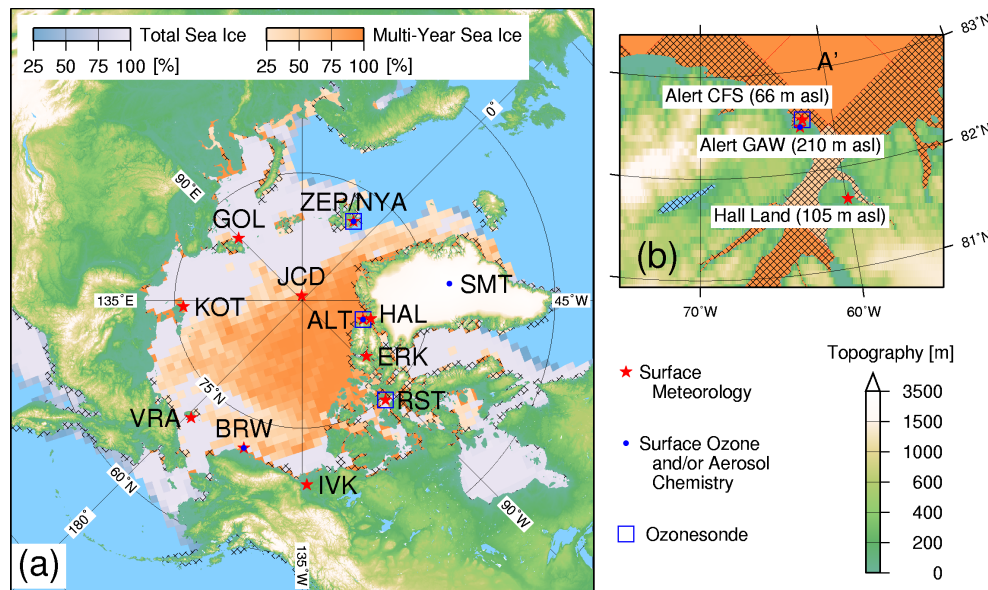


Fig. 2. (a) A map of observation sites for surface meteorology (red stars), surface ozone and aerosol chemistry (blue dots) and ozonesonde sounding (blue open squares) used for evaluating the present simulations. ALT: the Canadian Forces Station (CFS) and the Global Atmosphere Watch (GAW) station at Alert, Ellesmere Island, Canada (66 and 210 m a.s.l., respectively); BRW: Barrow NOAA/ESRL Observatory, Alaska, USA (8 m a.s.l.); ERK: Eureka, Ellesmere Island, Canada (10 m a.s.l.); GOL: Ostrov Golomjannyj, Russia (8 m a.s.l.); HAL: Hall Land, Greenland (105 m a.s.l.); IVK: Inuvik, Canada (68 m a.s.l.); JCD: J-CAD 3 drifting buoy deployed near the North Pole; KOT: Ostrov Kotelnjy, Russia (8 m a.s.l.); NYA: Ny Ålesund, Svalbard, Norway (18 m a.s.l.); RST: Rolute, Cornwallis Island, Canada (67 m a.s.l.); SMT: Summit, Greenland (3238 m a.s.l.); VRA: Ostrov Vrangeljja, Russia (5 m a.s.l.); and ZEP: Zeppelin, Svalbard, Norway (474 m a.s.l.). Also shown are the areas of higher than 25% sea-ice concentration from the CMC analyses (light purple shading) overlaid with the areas of higher than 25% multiyear sea-ice concentration from the QuikSCAT satellite data analyses (orange shading) for 15 April 2001, both of which are regridded to the horizontal resolution of the model. In areas with cross-hatching, snowpack on sea ice is assumed to act in the same fashion as that on land for air-snow bromine interactions in the model because grid-mean terrain height exceeds 50 m a.s.l. (see text); (b) A regional map focused on Alert CFS and GAW sites in Ellesmere Island, Canada and Hall Land in Greenland. For evaluating simulated ozone mixing ratios at Alert, model output at the grid cell A' adjacent to the nearest grid cell for the Alert CFS and GAW sites is also used.

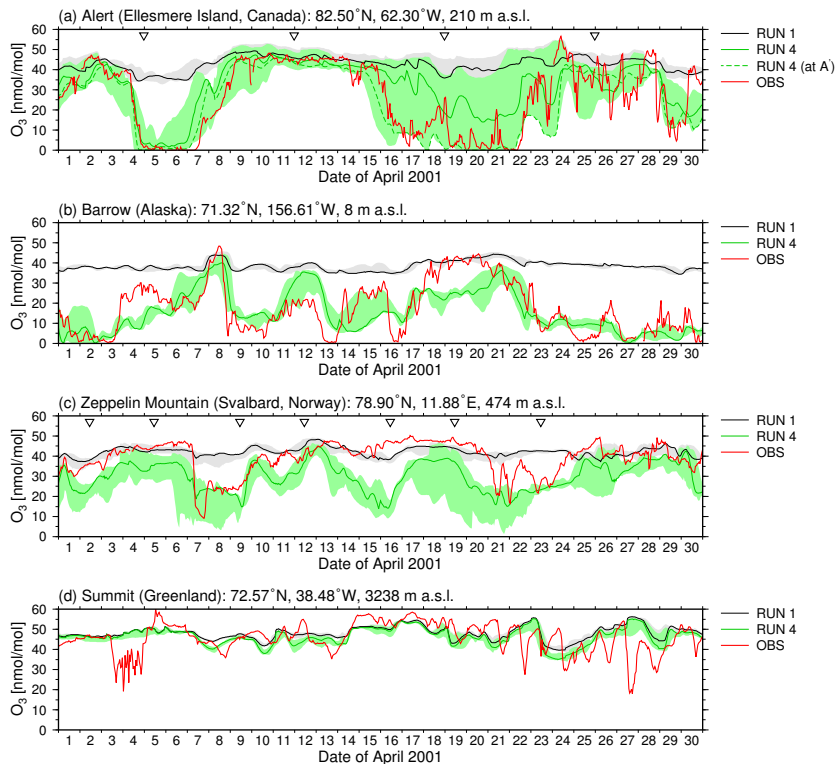


Fig. 3. (a) Comparison of surface ozone mixing ratios simulated in Run 1 (black line) and Run 4 (green lines) with those observed at Alert GAW station during April 2001. The solid line represents simulated time series at the nearest grid cell at the lowest model level with changes across the nearest and surrounding eight grid cells indicated by gray and light green shadings (for Run 1 and Run 4, respectively), whereas the red lines represent hourly observational data. Simulated time series from Run 4 include the dashed line representing ozone mixing ratios at the adjacent grid cell (location A' in Fig. 2b) at the third lowest vertical level of the model (~ 170 m a.s.l.); (b) the same as (a) but at Barrow; (c) the same as (b) but at Zeppelin. The model results at the nearest and surrounding grid cells are taken from the vertical levels containing the station level (474 m a.s.l.); and (d) the same as (b) but at Summit. Inverted triangles in (a) and (c) indicate the launching time of ozonesonde at Alert CFS and Ny Ålesund stations near Alert GAW and Zeppelin stations, respectively (see Fig. 6).

3-D modeling of Arctic boundary-layer bromine and ozone

K. Toyota et al.

Title Page

Abstract

Introduction

Conclusions

References

Tables

Figures

◀

▶

◀

▶

Back

Close

Full Screen / Esc

Printer-friendly Version

Interactive Discussion



3-D modeling of Arctic boundary-layer bromine and ozone

K. Toyota et al.

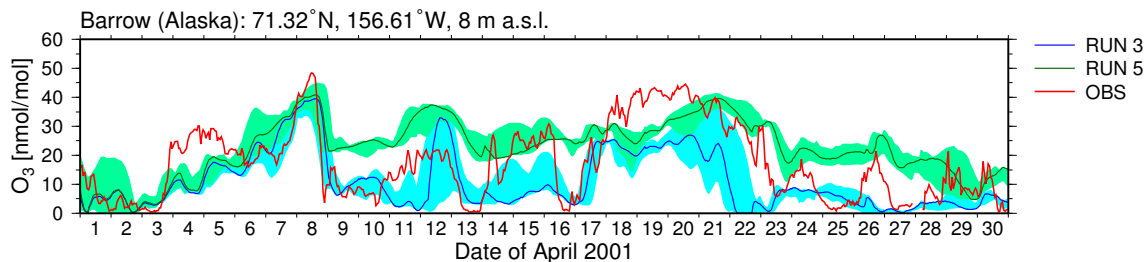


Fig. 4. The same as Fig. 3b but for simulated surface ozone mixing ratios at the nearest and surrounding grid cells to Barrow from Run 3 (blue line and shading) and Run 5 (green line and shading).

Title Page	
Abstract	Introduction
Conclusions	References
Tables	Figures
◀	▶
◀	▶
Back	Close
Full Screen / Esc	
Printer-friendly Version	
Interactive Discussion	



**3-D modeling of
Arctic boundary-layer
bromine and ozone**

K. Toyota et al.

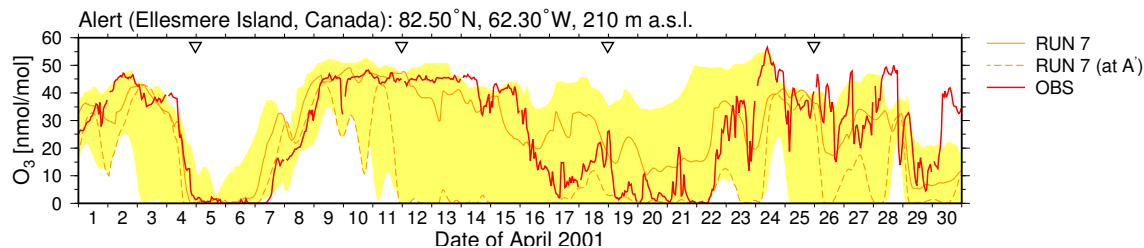


Fig. 5. The same as Fig. 3a but for simulated surface ozone mixing ratios at the nearest and surrounding grid cells to Alert from Run 7 (orange solid/dashed lines and yellow shading).

Title Page

Abstract

Introduction

Conclusions

References

Tables

Figures

◀

▶

◀

▶

Back

Close

Full Screen / Esc

Printer-friendly Version

Interactive Discussion



3-D modeling of Arctic boundary-layer bromine and ozone

K. Toyota et al.

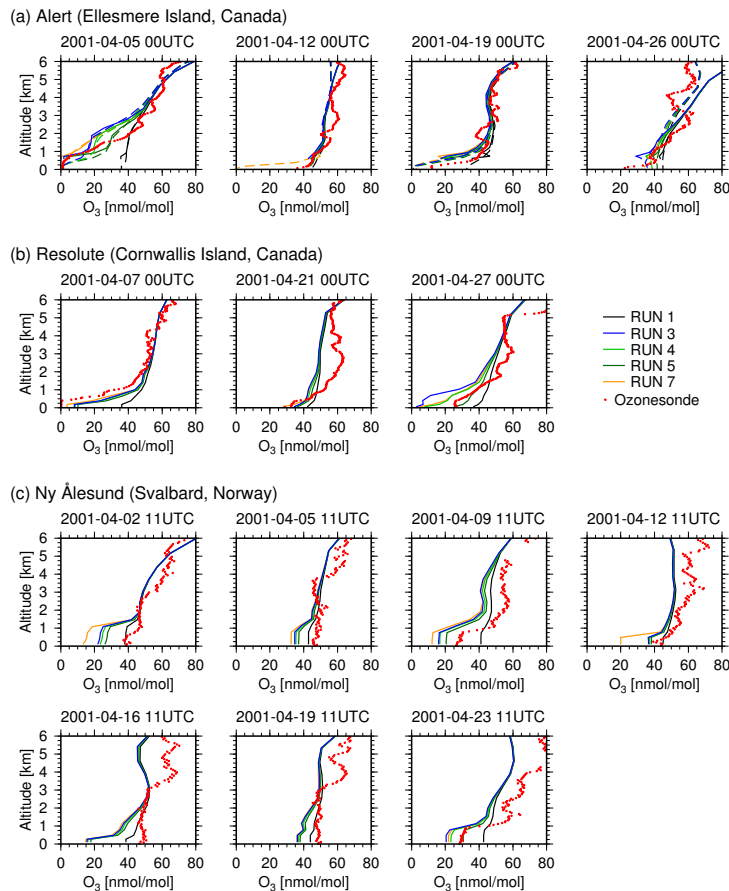


Fig. 6. (a) Comparison of simulated ozone profiles between 0–6 km a.s.l. for Run 1 (black lines), Run 3 (blue lines), Run 4 (light green lines), Run 5 (dark green lines) and Run 7 (orange lines) with observed profiles by ozonesonde (red dots) at Alert CFS. Solid lines are the simulated ozone mixing ratios at the nearest grid cell (with a grid-mean terrain height of 565 m a.s.l.) whereas dashed lines are those at one of the neighboring grid cells (location A' in Fig. 2b) with a grid-mean terrain height of 0 m a.s.l.; (b) the same as (a) but at Resolute. Simulated profiles are shown for the nearest grid cell only (solid lines); and (c) the same as (b) but at Ny Ålesund.

Title Page

Abstract

Introduction

Conclusions

References

Tables

Figures

◀

▶

◀

▶

Back

Close

Full Screen / Esc

Printer-friendly Version

Interactive Discussion



(a) GOME-SLIMCAT Tropospheric BrO VCD

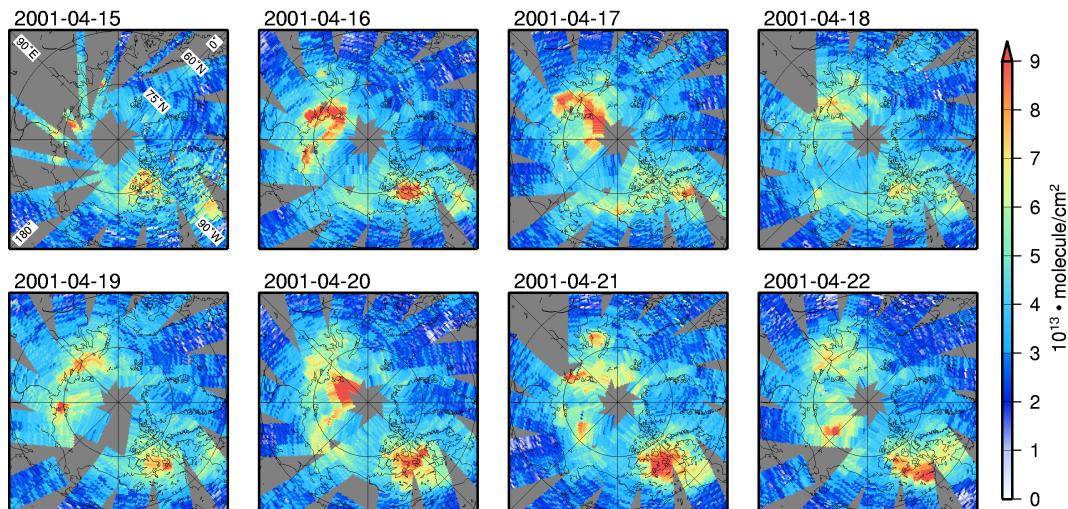


Fig. 7. (a) GOME-SLIMCAT tropospheric BrO VCDs (in molecule cm^{-2}) for each day between 15–22 April 2001; (b) The same as (a) but for BrO AVCDs (in molecule cm^{-2}) simulated by GEM-AQ in Run 3; (c) The same as (b) but simulated in Run 4; and (d) The same as (b) but simulated in Run 5. Note different color scales used for the GOME-SLIMCAT BrO VCDs and the GEM-AQ BrO AVCDs.

3-D modeling of Arctic boundary-layer bromine and ozone

K. Toyota et al.

Title Page

Abstract

Introduction

Conclusions

References

Tables

Figures

◀

▶

◀

▶

Back

Close

Full Screen / Esc

Printer-friendly Version

Interactive Discussion



3-D modeling of Arctic boundary-layer bromine and ozone

K. Toyota et al.

(b) GEM-AQ BrO AVCD (RUN 3: $T_c = -10^\circ\text{C}$, Net Bromine Release From FY Sea Ice Only)

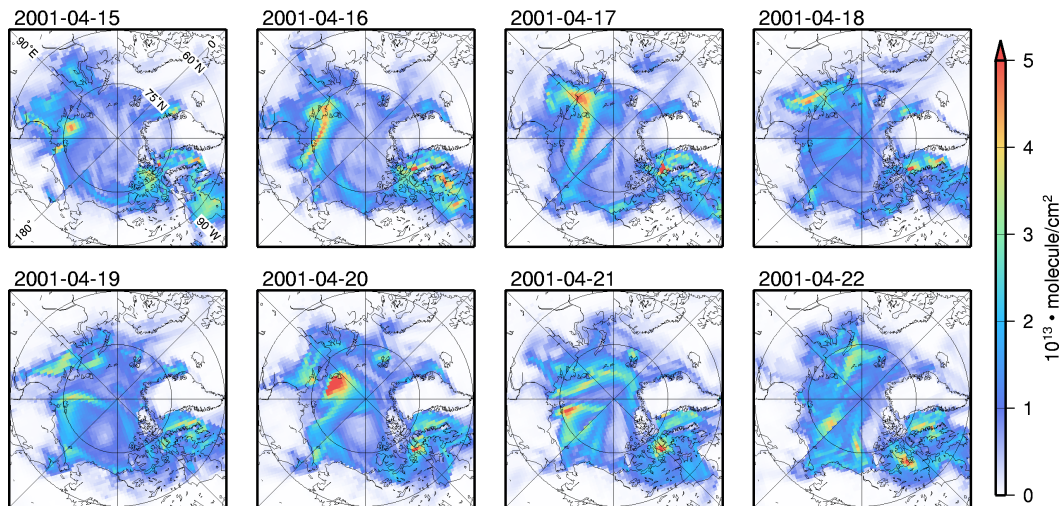


Fig. 7. Continued.

Title Page

Abstract

Introduction

Conclusions

References

Tables

Figures

◀

▶

◀

▶

Back

Close

Full Screen / Esc

Printer-friendly Version

Interactive Discussion



**3-D modeling of
Arctic boundary-layer
bromine and ozone**

K. Toyota et al.

Title Page

Abstract

Introduction

Conclusions

References

Tables

Figures

◀

▶

◀

▶

Back

Close

Full Screen / Esc

Printer-friendly Version

Interactive Discussion

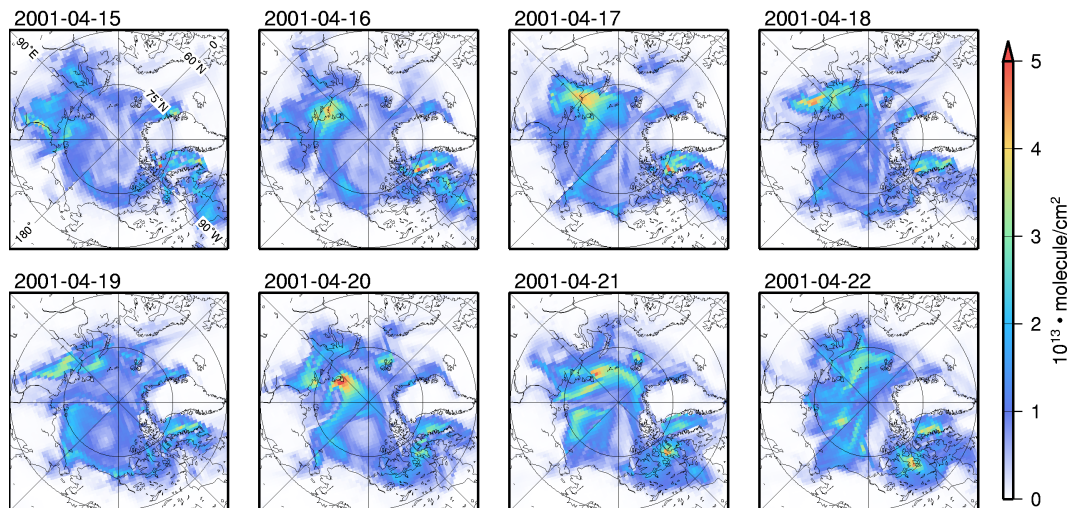
(c) GEM-AQ BrO AVCD (RUN 4: $T_c = -15^\circ\text{C}$, Net Bromine Release From FY Sea Ice Only)

Fig. 7. Continued.

**3-D modeling of
Arctic boundary-layer
bromine and ozone**

K. Toyota et al.

Title Page

Abstract

Introduction

Conclusions

References

Tables

Figures

◀

▶

◀

▶

Back

Close

Full Screen / Esc

Printer-friendly Version

Interactive Discussion

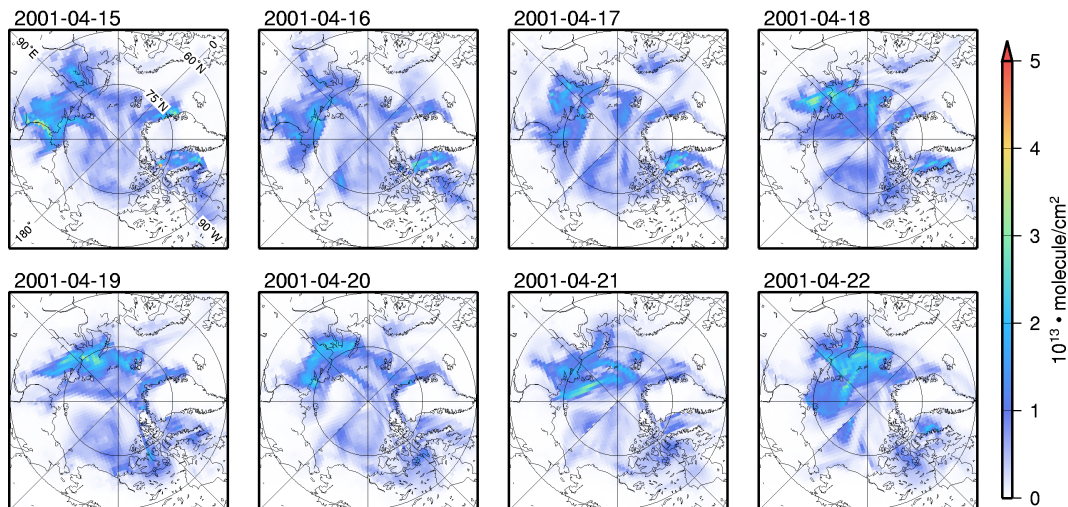
(d) GEM-AQ BrO AVCD (RUN 5: $T_c = -20^\circ\text{C}$, Net Bromine Release From FY Sea Ice Only)

Fig. 7. Continued.

3-D modeling of Arctic boundary-layer bromine and ozone

K. Toyota et al.

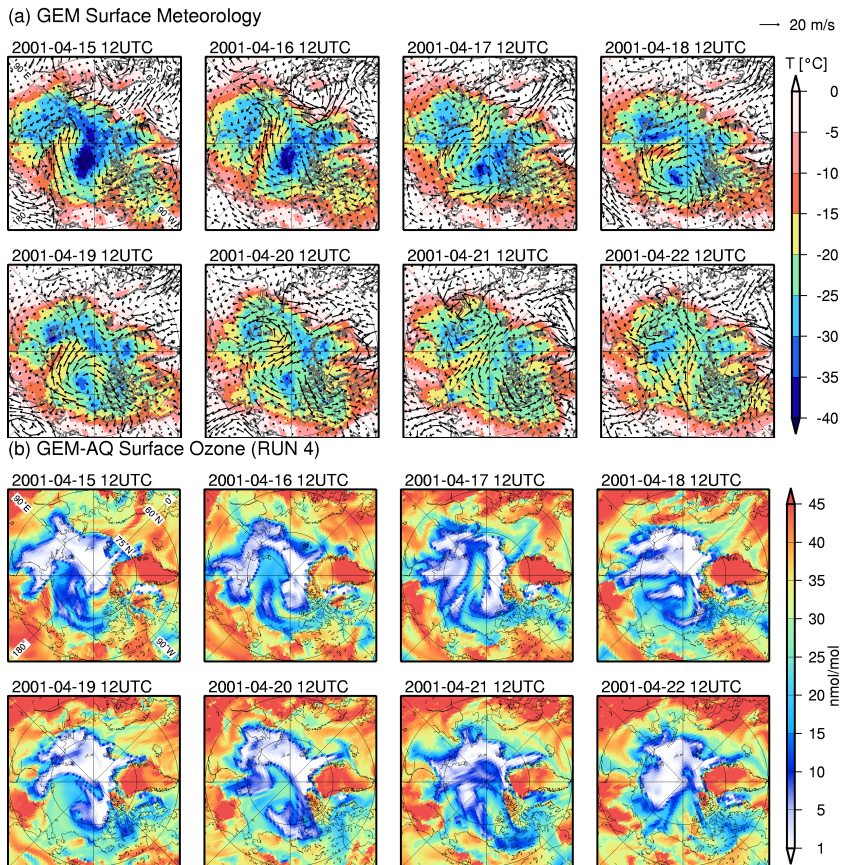
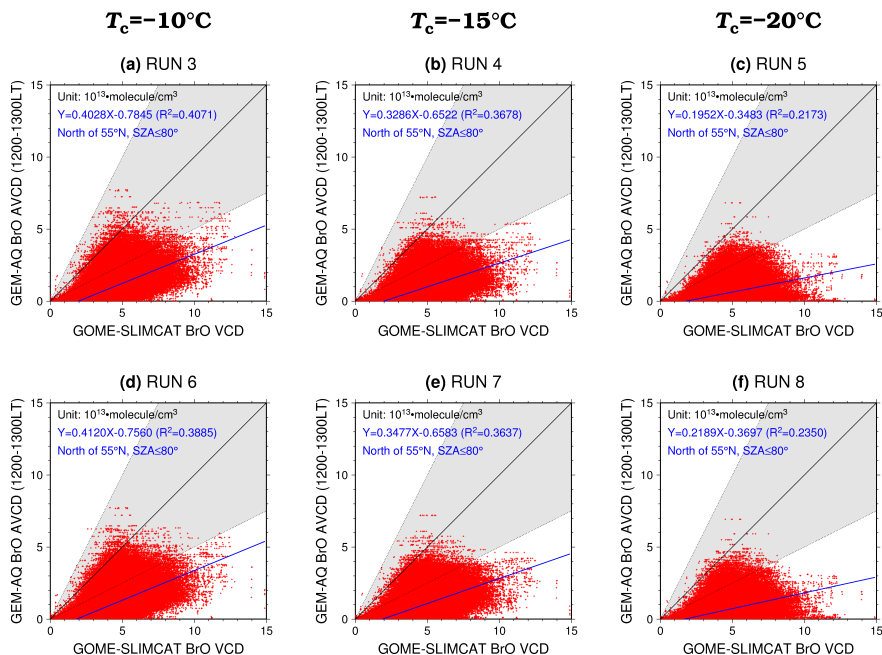


Fig. 8. (a) Surface air temperatures (color shade, in $^{\circ}\text{C}$) and wind vectors (arrow length for the wind speed of 20 m s^{-1} is indicated in the top right corner) at 12:00 UTC each day between 15–22 April 2001 simulated by the model; and (b) The same as (a) but for surface ozone mixing ratios (in nmol mol^{-1}) simulated in Run 4.

3-D modeling of Arctic boundary-layer bromine and ozone

K. Toyota et al.



**Net Bromine
Release From
FY Sea Ice
Only**

**Net Bromine
Release From
Both FY & MY
Sea Ice**

Fig. 9. Scatter plots of GEM-AQ BrO AVCDs versus GOME-SLIMCAT tropospheric BrO VCDs to the north of 55°N and for $\text{SZA} \leq 80^\circ$ during 1–30 April 2001. The GEM-AQ output (at the resolution of $0.88^\circ \times 0.88^\circ$ in the Arctic core) is regridded to $0.5^\circ \times 0.5^\circ$ used for the GOME-SLIMCAT dataset: **(a)** Run 3, **(b)** Run 4, **(c)** Run 5, **(d)** Run 6, **(e)** Run 7, and **(f)** Run 8.

Title Page

Abstract

Introduction

Conclusions

References

Tables

Figures

◀

▶

◀

▶

Back

Close

Full Screen / Esc

Printer-friendly Version

Interactive Discussion



3-D modeling of Arctic boundary-layer bromine and ozone

K. Toyota et al.

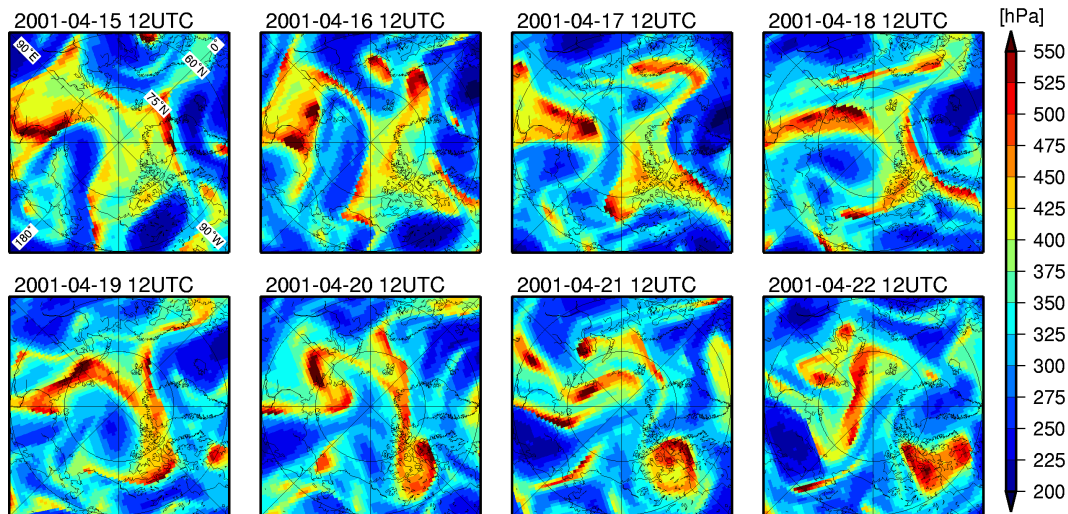


Fig. 10. Dynamical tropopause pressure levels (in hPa) defined by the 2 PVU surface at 12:00 UTC for each day between 15–22 April 2001 simulated by the GEM model.

[Title Page](#)[Abstract](#)[Introduction](#)[Conclusions](#)[References](#)[Tables](#)[Figures](#)[◀](#)[▶](#)[◀](#)[▶](#)[Back](#)[Close](#)[Full Screen / Esc](#)[Printer-friendly Version](#)[Interactive Discussion](#)

3-D modeling of Arctic boundary-layer bromine and ozone

K. Toyota et al.

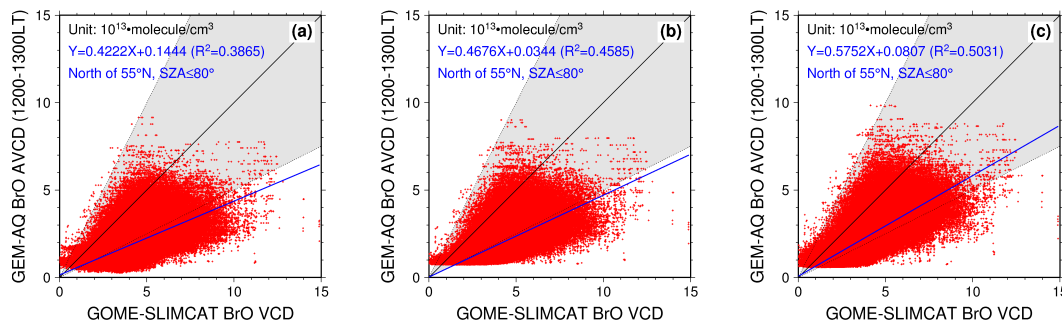


Fig. 11. The same as Fig. 9 but GEM-AQ BrO AVCDs from Run 3 are recalculated by adding extra BrO to the original model output: **(a)** 1 pmol mol^{-1} from the surface up to GEM's dynamical tropopause; **(b)** $0.5 \text{ pmol mol}^{-1}$ from the surface up to GEM's dynamical tropopause and 1 pmol mol^{-1} from the dynamical tropopause up to the 100 hPa level; and **(c)** $0.5 \text{ pmol mol}^{-1}$ from the surface up to GEM's dynamical tropopause and 3 pmol mol^{-1} from the dynamical tropopause up to the 200 hPa level.

Title Page

Abstract

Introduction

Conclusions

References

Tables

Figures

◀

▶

◀

▶

Back

Close

Full Screen / Esc

Printer-friendly Version

Interactive Discussion



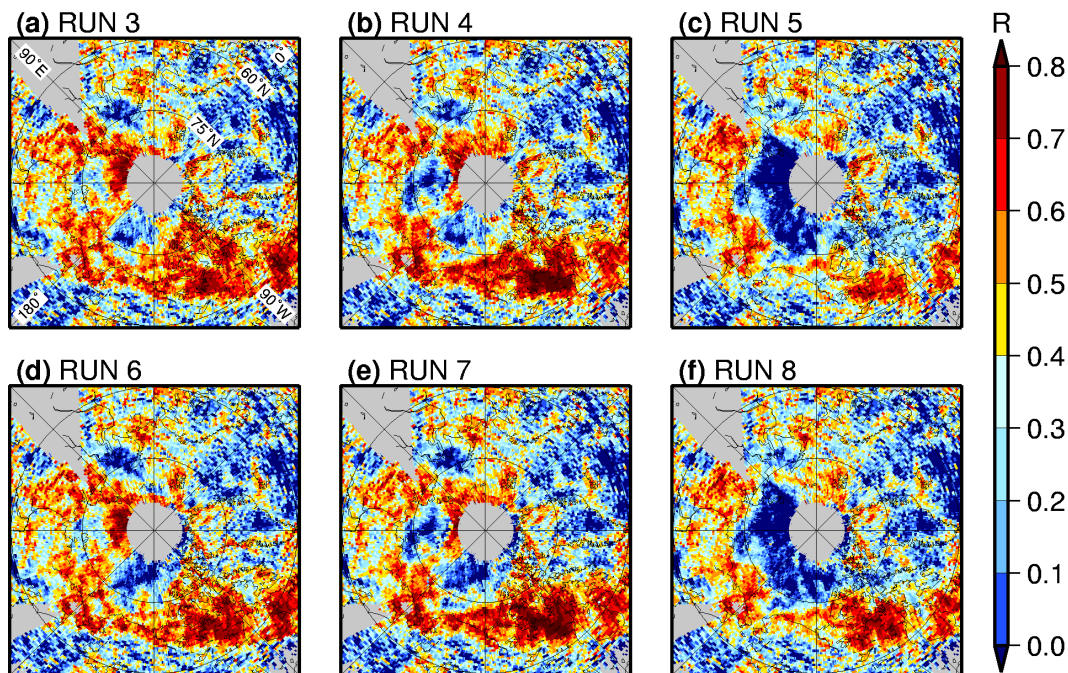


Fig. 12. Spatial distributions of temporal correlation coefficients between GEM-AQ BrO AVCDs and GOME-SLIMCAT tropospheric BrO VCDs in April 2001: **(a)** Run 3, **(b)** Run 4, **(c)** Run 5, **(d)** Run 6, **(e)** Run 7, and **(f)** Run 8. The GEM-AQ output (at the resolution of $0.88^\circ \times 0.88^\circ$ in the Arctic core) is regridded to $0.5^\circ \times 0.5^\circ$ used for the GOME-SLIMCAT dataset. Shaded by gray where the number of samples is less than 16.

3-D modeling of Arctic boundary-layer bromine and ozone

K. Toyota et al.

Title Page

Abstract Introduction

Conclusions References

Tables Figures

◀ ▶

◀ ▶

Back Close

Full Screen / Esc

Printer-friendly Version

Interactive Discussion



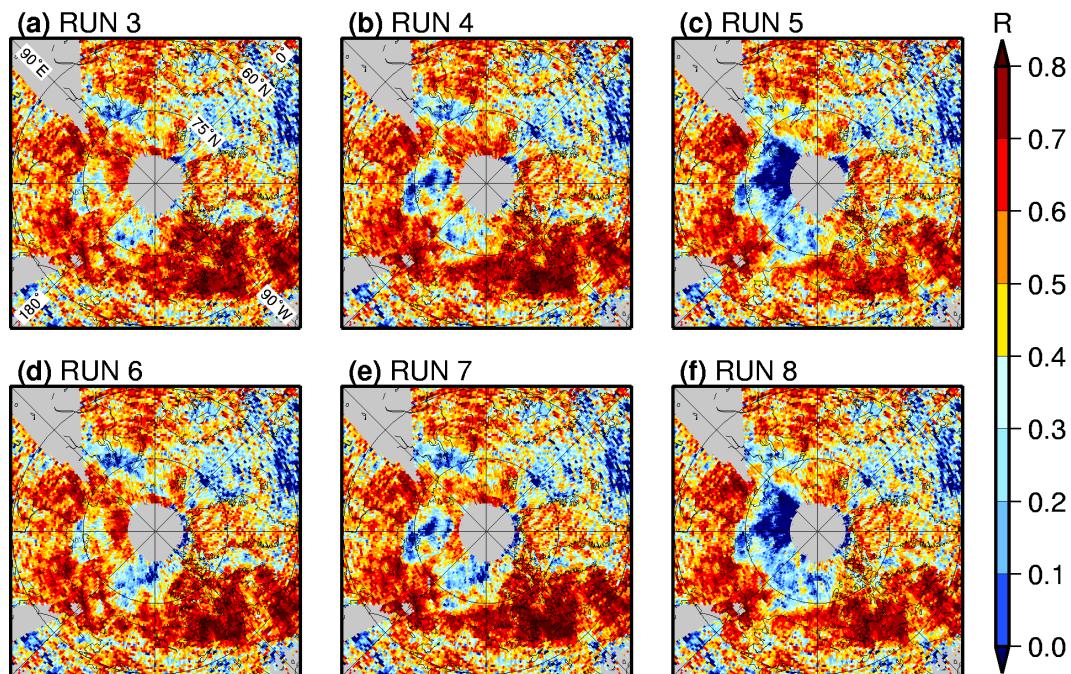


Fig. 13. The same as Fig. 12 but for GEM-AQ BrO AVCDs recalculated by adding extra BrO to the original model output, $0.5 \text{ pmol mol}^{-1}$ from the surface up to GEM's dynamical tropopause and 3 pmol mol^{-1} from the dynamical tropopause up to the 200 hPa level.

[Title Page](#)[Abstract](#)[Introduction](#)[Conclusions](#)[References](#)[Tables](#)[Figures](#)[◀](#)[▶](#)[◀](#)[▶](#)[Back](#)[Close](#)[Full Screen / Esc](#)[Printer-friendly Version](#)[Interactive Discussion](#)

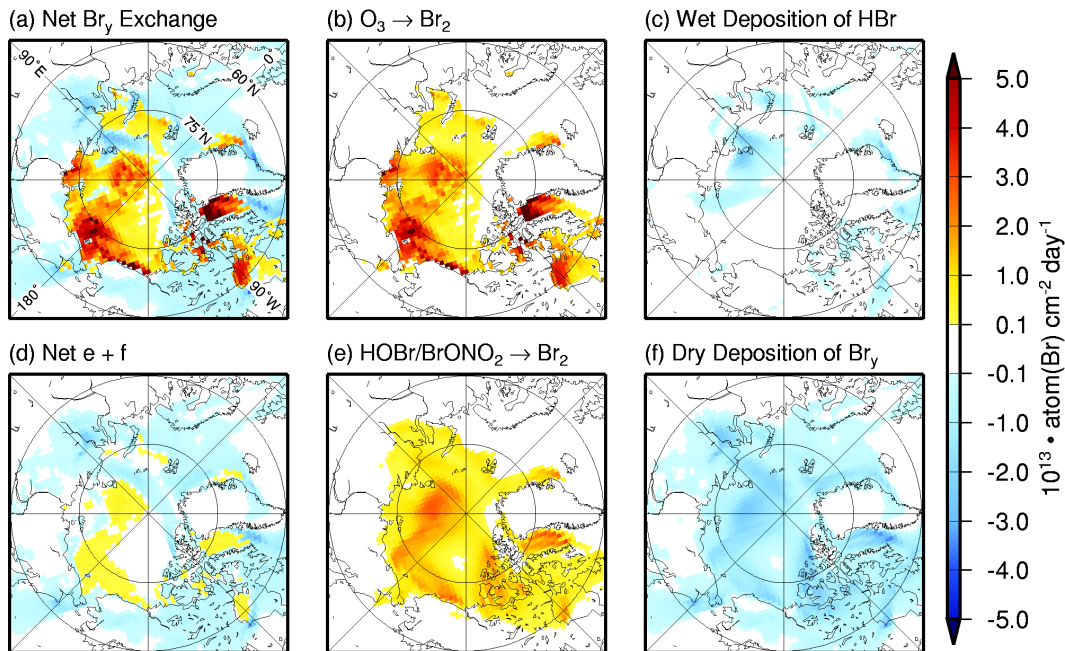


Fig. 14. The rate of bromine exchange between the atmosphere and the Earth surface integrated over 24 h between 00:00–24 UTC on 20 April 2001 as simulated in Run 3, as well as the breakdown of contributing mechanisms: **(a)** The total net exchange of all the inorganic bromine species; **(b)** Br_2 release via dry deposition of ozone on the FY sea ice; **(c)** Wet deposition of HBr integrated over the atmospheric column; **(d)** The net rate of air-surface bromine exchange via “explosion” chemistry as represented by the sum of **(e)** and **(f)**; **(e)** Br_2 release via dry deposition of HOBr and BrONO_2 ; and **(f)** Dry deposition of all the inorganic bromine species. Positive values represent a net release to the atmosphere whereas negative values represent a net loss from the atmosphere (in $\text{atom}(\text{Br}) \text{cm}^{-2} \text{day}^{-1}$).

3-D modeling of Arctic boundary-layer bromine and ozone

K. Toyota et al.

Title Page	
Abstract	Introduction
Conclusions	References
Tables	Figures
◀	▶
◀	▶
Back	Close
Full Screen / Esc	
Printer-friendly Version	
Interactive Discussion	

